MICROCOPY RESOLUTION TEST CHART

NATIONAL BUREAU OF STANDARDS 1963-A
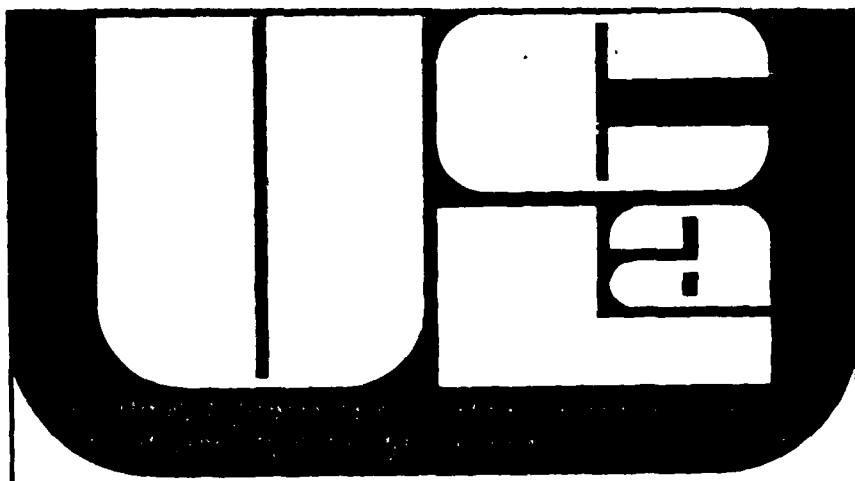
①

DTIC
SELECTE**D**
AUG 2 8 1987
C&D

SELF-CONSISTENT MODIFICATION OF A FAST TAIL

DISTRIBUTION BY RESONANT FIELDS IN

NONUNIFORM PLASMAS

G. J. Morales, M. M. Shoucri, J. E. Maggs

August, 1987   PPG-1089

CENTER FOR
PLASMA PHYSICS
AND
FUSION ENGINEERING

UNIVERSITY OF CALIFORNIA
LOS ANGELES

8 25 080

DTIC

SELECTE**D**

AUG 2 8 1987

C&**D**

SELF-CONSISTENT MODIFICATION OF A FAST TAIL
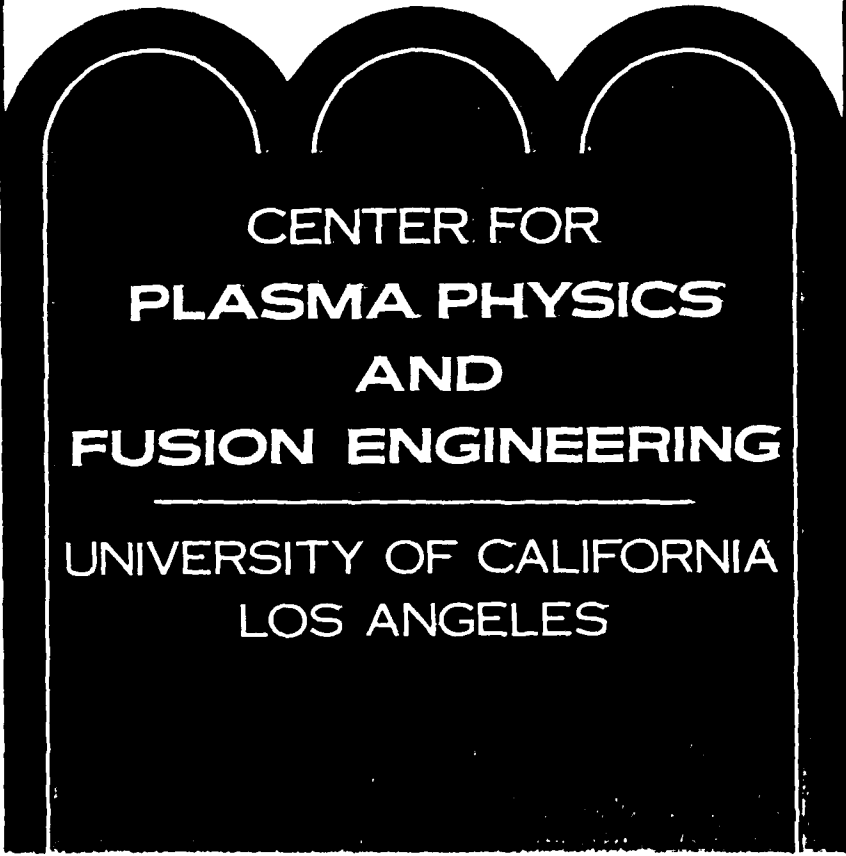
DISTRIBUTION BY RESONANT FIELDS IN

NONUNIFORM PLASMAS

G. J. Morales, M. M. Shoucri, J. E. Maggs

August, 1987   PPG-1089

University of California

Department of Physics

Los Angeles, CA 90024

Self - Consistent Modification of a Fast Tail Distribution by

Resonant Fields in Nonuniform Plasmas

G. J. Morales, Merit M. Shoucri, and J. E. Maggs

Physics Department, University of California at Los Angeles
Los Angeles, California 90024-1547

Abstract

An analytic study is made of the second order modifications produced on
the fast tail electron distribution function of a nonuniform plasma subjected
to resonant excitation by wave sources. The source models considered can
represent excitation by external electromagnetic waves propagating obliquely
to the plasma density gradient, mode-conversion of electrostatic whistlers,
beat of two transparent electromagnetic waves, and direct conversion from
ripples in the density profile. The calculation treats the Landau damping
provided by fast tail electrons self-consistently and is applicable to plasmas
having a long density scale length L, i.e., $(k_D^7 L)^{1/3} \gg 1$, where k_D is the
Debye wave number of the warm background electrons. A threshold condition is
found for the formation of a positive slope in the tail distribution by the
various excitation mechanisms.

PACS - 52.25 Fi, 52.35 Nx, 52.40 Mk

I. Introduction

The modification of the zero order electron velocity distribution function by resonantly excited waves is a central problem encountered in various plasma physics applications, e.g., ionospheric modification, laser fusion, and RF heating. In some cases it is possible, because of certain parameter orderings, to decouple the calculation of the modified distribution function from the determination of the spatial shape of the driven electric field causing the modification. Such an approach is physically meaningful if the density of resonant particles is small enough that their contribution to the total energy and momentum balance, due to Landau damping, can be considered to be a small perturbation, i.e., the resonant particles behave as test particles. An example of this type of non-self-consistent calculation has been recently reported[1] by the authors in a study of resonant absorption of radio waves in an ionosphere in which a small photoelectron population is present. In that earlier study the shape of the modulus of the resonant electric field (and hence the wave spectrum) is predominantly determined by collisions of the background (slow) electrons because, for typical ionospheric conditions, the effective phase velocity at the resonance layer (where the external frequency ω matches the local electron plasma frequency $\omega_p(z)$) is quite large compared to the thermal velocity of the background electrons. Hence, the modifications in the distribution function can be calculated, for large velocities, by using the collisionally limited spectrum, as described in detail in Ref. 1.

In the present study we report a self-consistent calculation, accurate to second order in the electric field amplitude, of the time-averaged modification produced on a pre-existing fast electron tail distribution by resonantly excited electric fields in a nonuniform plasma. Two different methods of

excitation covering a wide range of physically realizable configurations
are considered: one is a capacitor-like pump field (wave number $k_0 = 0$), and
the other is a unidirectional beat-type exciter having finite wave number
($k_0 \neq 0$). The $k_0 = 0$ source models the external excitation by electromagnetic
waves propagating obliquely to a density gradient, as well as the internal
excitation by obliquely propagating electrostatic whistler waves[2], as may
occur naturally in the topside polar ionosphere, or may result from a signal
launched from a spacecraft. The $k_0 \neq 0$ source models the external pumping
that can be produced by the beat of two transparent electromagnetic waves
having frequencies ω_1, ω_2 such that ω_1, $\omega_2 \gg \omega_p$, but $\omega_2 - \omega_1 \sim \omega_p$, as is
presently being considered in laser accelerator schemes[3]. This type of source
can also model the beat pumping resulting naturally when an external electro-
magnetic wave interacts with a pre-existing low frequency ripple in the
density profile, i.e., the process known as direct conversion[4,5]. The finite
k_0 exciter can also be related to interactions stimulated by modulated beams,
to truncated velocity distribution functions, and to single particle Cerenkov
emission.

A consequence of the results reported here is that the study of Ref. 1
can be generalized to conditions in which a sizeable fast electron population
(e.g., large photoelectron flux) is present. In addition, it is hoped that
the present study may be useful for undertaking more general studies (both
theoretical and experimental) of wave-particle interactions in nonuniform
plasmas since a wide class of excitation mechanisms is treated self-
consistently.

It is worth emphasizing that an extensive literature[6-11] exists on the
topic of hot electron production in laser fusion experiments. Numerous
studies have demonstated that in such experiments fast electron tail

distributions are generated by intense electrostatic oscillations driven at plasma resonance. A related issue which is presently being debated by experts in this field is whether or not some spectral features observed in the backscattered laser light are attributable[12] to distortions in the fast tail distribution. Although the present study does not consider the extreme short density scale length environment appropriate for laser experiments, we report here on the amplitude threshold condition required (according to second order perturbation theory) to create a positive slope on the velocity distribution function of a long density scale length plasma in which a zero order energetic electron component is present. We note further that various aspects of this problem, akin to some issues discussed here, have been recently examined by Colunga, et al.[13], for the laser relevant case of short scale length.

The physical model examined in the present study consists of a one-dimensional, warm fluid background plasma having a zero order density profile $n_0(z)$, which can be well approximated in the neighborhood of the plasma resonance by a linear function of position, i.e., $d\ln n_0(z)/dz = L^{-1}$ for $\omega_p(z) \approx \omega$. The plasma is subjected to external pumping by an effective electric field of the form $E_0 \exp[i(k_0 z - \omega t)]$ and three physically different situations ($k_0 = 0$, $k_0 > 0$, $k_0 < 0$) are investigated. A spatially uniform population of energetic electrons is assumed to be present with density n_t small compared to that of the background plasma, i.e., $n_t/n_0 \ll 1$. The separation of the background scale length L from that of the tail electrons (i.e., $L_t \to \infty$) is physically meaningful because of the large disparity between the collision lengths of the background and tail particles. Also, the fast particle collision length is much larger than the scale length of the resonant field structures generated at $\omega_p(z) = \omega$. Such ordering of scale

lengths is naturally achieved in a wide range of plasma environments, e.g., laboratory discharge plasmas and the ionosphere.

For illustrative purposes, in the discussion of the effects produced by a spatially uniform source ($k_0 = 0$) we emphasize two extreme limits of the resonantly excited electric fields. One is the collisionally dominated Lorentzian shape, and the other is the convectively limited driven-Airy waveform. Of course, we also consider the general problem that includes collisions, convection, and Landau damping by fast electrons. To obtain a physical understanding of the relevant parameter scalings entering in the various cases considered here, we recall that the collisionally dominated plasma resonance exhibits a peak electric field given by (ω/ν) E_0, a characteristic spatial width, (ν/ω) L, and an effective resonant velocity $v_L = (\nu/\omega)\omega L$, where ν is the collision frequency of the background plasma electrons. In contrast with this ordering the convectively limited resonance (for $k_0 = 0$) has peak electric field amplitude $(k_A L)$ E_0, characteristic scale length at plasma resonance k_A^{-1}, and effective particle resonant velocity at plasma resonance $v_A \sim \omega/k_A$, where $k_A \equiv (k_D L/\sqrt{3})^{2/3}$ L^{-1}, and $k_D = \omega/\bar{v}$ is the Debye wave number of the background plasma whose thermal velocity is $\bar{v}$.

It then follows that the collisionally dominated resonance is operative if $(k_D L/\sqrt{3})^{2/3} \gg \omega/\nu$, in which case the velocity of those fast electrons that can be significantly modified by the resonance must be comparable to v_L and satisfies $v_L/\bar{v} \gg (k_D L/\sqrt{3})^{1/3}$. Convective limitation of the plasma resonance begins to appear for $(k_D L/\sqrt{3})^{2/3} \sim \omega/\nu$, and implies that the resonant electron population that can be affected must have velocities $v_A/\bar{v} \sim (k_D L/\sqrt{3})^{1/3}$. Thus, for the two extreme limits of resonant amplitude limitation the strong wave-particle interactions are anticipated to arise from electrons having velocities on the order of $(k_D L/\sqrt{3})^{1/3} \bar{v}$, which can be large

for systems with large $k_D L$, as is the case for ionospheric and space plasmas. It is this population in velocity space that we refer to as the fast tail. It is the goal of the present study to calculate the modifications produced in this velocity interval to second order in the amplitude of the self-consistent resonant electric fields.

The manuscript is organized as follows. Section II describes the self-consistent calculation of the resonant electric fields. The second order modification of the tail distribution and the threshold for positive slope development are considered in Sec. III. A summary of results and conclusions are presented in Sec. IV.

II. Self - Consistent Fields

The geometry of the one-dimensional problem being considered is sketched in Fig 1. The location $z = 0$ corresponds to the resonant layer $\omega_p = \omega$ and the density scale length of the background plasma is introduced through $1 - \omega_p^2(z)/\omega^2 = z/L$, where z is the independent variable. In configuration space the complex amplitude $E(z)$ of the self-consistent electric field driven by an effective source field $E_0 S(z) \exp(-i\omega t)$ (with $S(z)$ representing the various pumping schemes) is determined from Poisson's equation, whose exact form is an integral equation of the type

$$\int_{-\infty}^{\infty} dz' \, K(z',z,\omega) \, E(z') = E_0 \, S(z) \quad , \tag{1}$$

in which $K(z', z, \omega)$ is a kernel derived by integrating the Boltzmann equation, but whose detailed structure need not be analysed here. By expanding the kernel in terms of the ratio of the background thermal velocity $\overline{v}$ to the effective phase velocity of the field (i.e., the quantity v_A discussed earlier), Eq. (1) is approximated in the lowest order by

$$\epsilon(z,\omega)E(z) = E_o\, S(z) \quad , \quad (2)$$

in which the local dielectric operator takes the form

$$\epsilon(z,\omega) = \frac{3}{k_D}2\frac{d^2}{dz^2} + \frac{z}{L} + i\Gamma \quad , \quad (3)$$

where $\Gamma = \nu/\omega$. Equation (3) does not contain the Landau damping contribution of the background electrons because for the case of interest here, namely $(k_{DL})^{1/3} \gg 1$, it is negligible since it scales as $\exp[-(k_{DL}/\sqrt{3})^{2/3}/2]$. However, we are interested in describing effects resulting from wave-particle resonances with a spatially uniform tail population whose density is small enough that the location of the cold plasma resonance due to the background electrons is not affected. To include the Landau damping caused by the tail population we return to the general form of Eq. (2) and express it in Fourier space, namely

$$[\frac{i}{L}\frac{d}{dk} + i\Gamma - \frac{3k^2}{k_D^2} + i4\pi\ \mathrm{Im}\ \tilde{\chi}_t]\ \tilde{E}(k) = E_o\ \tilde{S}(k) \quad , \quad (4)$$

where

$$\tilde{E}(k) = \int_{-\infty}^{\infty} dz\ e^{-ikz}\ E(z) \quad , \quad (5)$$

and with a similar definition for $\tilde{S}(k)$.

In Eq. (4) the Fourier transform of the dielectric operator now contains the important imaginary part arising from the susceptibility of the tail electrons $\tilde{\chi}_t(k)$. For a model Maxwellian tail distribution having the form

$$f_{ot}(v) = \frac{n_t}{(2\pi v_t^2)^{1/2}}\ \exp(-v^2/2v_t^2) \quad , \quad (6)$$

$$4\pi \text{Im} \, \tilde{\chi}_t(k) = (\frac{k_{Dt}}{k})^2 \, (\frac{\pi}{2})^{1/2} \, \frac{\omega}{kv_t} \exp(-\omega^2/2k^2v_t^2) \quad , \tag{7}$$

where $k_{Dt} = k_D \, (\overline{v}/v_t)\sqrt{\Delta}$ is the tail Debye wave number and $\Delta \equiv n_t/n_0(0)$. A useful feature of Eq. (7) is that

$$4\pi \text{Im} \, \hat{\chi}_t(k) = \frac{d}{dk} g(k)$$

$$g(k) = \Delta(\frac{\overline{v}}{v_t}) \, k_D \, (\frac{\pi}{2})^{1/2} \, \exp(-\omega^2/2k^2v_t^2) \quad , \tag{8}$$

hence, Eq. (4) becomes

$$\frac{i}{L} \frac{d}{dk} \tilde{E}(k) + \{i \frac{d}{dk} [\Gamma k + g(k)] - \frac{3k^2}{k_D^2}\}\tilde{E}(k) = E_o \, \tilde{S}(k) \quad , \tag{9}$$

which is solved by defining $\hat{E}(k) \equiv \exp[F(k)]a(k)$, with

$$F(k) = -i \frac{k^3 L}{k_D^2} - [\Gamma k + g(k)]L \quad , \tag{10}$$

to obtain

$$\frac{d}{dk}a(k) = -iE_oL\tilde{S}(k)\exp[-F(k)] \quad . \tag{11}$$

The three different excitation schemes of interest here are contained in the choice $\tilde{S}(k) = 2\pi\delta(k - k_o)$, with $k_o = 0$, $k_o > 0$, $k_o < 0$. Hence, Eq. (11) can be integrated to yield

$$\hat{E}(k) = -2\pi iE_oL\theta(k - k_o)\exp[F(k)-F(k_o)] \quad , \tag{12}$$

in which $\theta(k - k_o)$ refers to the Heaviside unit step function. In Eq. (12) the boundary condition $a(-\infty) = 0$ has been chosen because, due to evanescence, no waves propagate to $z = -\infty$.

A. Uniform Pump

Inserting the value $k_0 = 0$ in Eq. (12) yields the electric field spectrum excited by a capacitor - like pump field. The spectrum is unidirectional (i.e., $k > 0$) because the waves are excited at cut-off. In discussing this pumping scheme it is useful to isolate two extreme limits: in one the amplitude is limited by collisions and results in a Lorentzian shape in configuration space, while in the other the resonance is limited by convection and exhibits a driven - Airy pattern. The corresponding spectra are:

$$\tilde{E}_L(k) = 2\pi E_0 \theta(k) \exp[-i\frac{\pi}{2} - \frac{k}{k_L} - \alpha \exp(-k_t^2/k^2)] , \tag{13}$$

$$\tilde{E}_A(k) = 2\pi E_0 \theta(k) \exp[-i\frac{k^3}{3k_A^3} -i\frac{\pi}{2} - \frac{k}{k_L} - \alpha \exp(-k_t^2/k^2)] , \tag{14}$$

where $k_L = (\Gamma L)^{-1}$ is the characteristic wave number of the Lorentzian resonance, $k_A = (k_D L/\sqrt{3})^{2/3} L^{-1}$, $\alpha = (\pi/2)^{1/2} \Delta k_D L (\bar{v}/v_t)$ is the scaled tail density, and $k_t = \omega/(\sqrt{2} v_t)$ is the characteristic wave number of the tail particles. Note that Eq. (13) follows from Eq. (14) in the limit $(k_L/k_A)^3 \ll 3\pi/2$.

An interesting feature of Eqs. (13) and (14) is that $|\tilde{E}_L(k)|^2 = |\tilde{E}_A(k)|^2$, hence second order phase-independent effects caused by these two fields are identical although their spatial patterns can be quite different. In particular the time - averaged modification of the tail distribution function, accurate to order $|E_0|^2$, is the same for the collisionally and the convectively limited resonances.

Figure 2 exhibits two complementary dependences of the scaled modulus of the spectrum for a collisionally dominated resonance (i.e., k_L/k_A small). The broken curves correspond to the dependence of $|\tilde{E}(k)|$ on scaled wave number (top scale) while the solid curves (more useful in understanding wave - particle

interactions) show the dependence on resonant particle velocity (i.e., $v = \omega/k$) scaled to the tail velocity v_t for $k_L/k_A = 0.25$ and $k_t/k_A = 6$. We remark parenthetically that in plotting the modulus of $\tilde{E}(k)$, k_A does not appear explicitly but we scale to this variable for convenience in the latter analysis. The curves labelled $\alpha = 0$ are determined by collisional damping alone, and the rest contain the effect of self-consistent Landau damping. The sequence of solid curves illustrates the role of increasing tail density from $\alpha = 0$ to 50 for fixed k_L/k_A (for instance if $k_D L \sim 10^4$, $\bar{v}/v_t \sim 10^{-1}$, $\alpha = 50$ corresponds to a tail density ratio of .04). It is seen from Fig. 2 that the principal effect of self-consistency is to prevent the acceleration of slower tail electrons due to the quenching of the large k components of the spectrum. This quenching results also in a steepening of the spectrum as a function of velocity, i.e., $\partial |\tilde{E}(k = \omega/v)|/\partial v$ increases. Such an effect can result in a strong distortion of the distribution function over a limited velocity range, as is shown in Sec. III.

The spatial dependence of the self-consistent fields is obtained from the inverse Fourier transform

$$E(z) = \frac{1}{2\pi} \int_{-\infty}^{\infty} dk \; \tilde{E}(k) e^{ikz} \quad , \tag{15}$$

which is evaluated numerically for the spectra of Eqs. (13) and (14) to yield the results of Figs 3 and 4, respectively.

Figure 3 displays the spatial pattern associated with a collisionally limited resonance (i.e., systems with $(k_D L/\sqrt{3})^{2/3} \gg \omega/v$). The $\alpha = 0$ curve corresponds to $E(z)/(E_0 L) = (z + i\Gamma L)^{-1}$, which is the cold plasma resonance, while the curve labelled $\alpha = 10$ shows the effect of self-consistency for $k_L/k_t = \sqrt{3}$. It is seen that Landau damping by the fast tail decreases the peak amplitude of the collisional resonance, i.e., an increased effective

dissipation rate results whose magnitude can be approximately estimated from Eq. (13) by setting $k = k_L$ to yield $\Gamma \rightarrow \Gamma \left\{1 + \alpha \exp\left(-(\Gamma k_t L)^2\right)\right\}$. Another effect is the appearance of oscillatory features in the wings of the electric field modulus.

The spatial pattern of the convectively limited resonance is exhibited in Fig. 4, where the scaled modulus of the electric field $|E_A(z)|/k_A L E_0$ is plotted versus the scaled spatial coordinate $\zeta = k_A z = (k_D L/\sqrt{3})^{2/3} z/L$. The curve labelled $\Gamma' = 0$, $\alpha = 0$, corresponds to the undamped mode conversion result[14] $\pi|Gi(-\zeta) + i\, Ai(-\zeta)|$, while the curve labelled $\Gamma' = 0.25$, $\alpha = 0$, exhibits the effect of collisional damping and is given by $\pi|Gi(-\zeta+i\Gamma')| + i\, Ai(-\zeta+i\Gamma')$ where Gi, Ai represent the appropriate Airy-type functions[15], and $\Gamma' = k_A/k_L = (k_D L/\sqrt{3})^{2/3}(\nu/\omega)$ is the scaled damping. The bottom curve in Fig. 4 contains the combined effects of collisions and tail Landau damping for $\Gamma' = 0.25$, $\alpha = 10$, and $(k_t/k_A)^2 = 40$. It is seen from this curve that at this relatively low tail particle density the peak amplitude of the resonance is not affected by Landau damping, but that a reduction due to collisional dissipation occurs. For the conditions chosen in Fig. 4, tail Landau damping begins to overwhelm collisional damping of the mode-converted Langmuir wave beyond the third oscillation of the Airy pattern. It is expected that at this spatial location the distortions in the distribution function calculated in Sec. III begin to appear.

For completeness we would like to add that the connection between the amplitude E_0 entering into the $k_0 = 0$ model discussed here and the power per unit area P_0 carried by an electromagnetic wave approaching plasma resonance from the low density side at an asymptotic angle θ is

$$|E_0| = \left(\frac{8\pi P_0}{\omega L}\right)^{1/2} \quad , \tag{16}$$

where η is the mode conversion absorption efficiency determined by Kelly and
Bancs[16], and by Fordslund, et al.[17], and which for small q values behaves[18] as
$\eta = a(q-2aq/3)$, with $a \approx 2.6$, and where $q \equiv (\omega L/c)^{2/3} \sin^2\theta$, with c the
speed of light.

The corresponding connection between E_0 and the asymptotic amplitude E_w
of an obliquely propagating electrostatic whistler wave with frequency ω
smaller than the electron gyrofrequency Ω , and approaching plasma resonance
along $\underline{B}_0$ from the high density side of a magnetized plasma with $\nabla n_0 \times \underline{B}_0 = 0$
is

$$E_0 = \frac{E_w}{\sqrt{\pi}} \left[\cosh(\pi\beta_0)\right]^{1/2} e^{-\pi\beta_0} , \tag{17}$$

where $\beta_0 \equiv (k_\perp L)Y^2/\left[2(Y^2-1)^{1/2}\right]$, with $Y = \Omega/\omega$ and $k_\perp$ is the constant
wave number perpendicular to the confining field $\underline{B}_0$.

B. Beat Excitation

We proceed to examine the resonant excitation of plasma waves by $k_0 \neq 0$
sources, as may arise from various beat processes. For example, beat excita-
tion by two transparent electromagnetic waves propagating along the density
gradient in an unmagnetized plasma and having frequencies ω_1, ω_2 , with $\omega_2-\omega_1$
$\approx \omega_p(0)$, causes a beat-ponderomotive force on the background electrons. The
value of the effective field E_0 entering in Eq.(13) is then given by

$$E_0 = -\frac{e}{mc}\frac{\omega_p(0)}{\omega_1\omega_2} |E_{01}E_{02}|\exp[i(\theta_2-\theta_1)] , \tag{18}$$

where e, m are the electron charge and mass, E_{0j} represents the amplitude of
the jth electromagnetic wave, and θ_j is the corresponding phase. If the
excitation results from the beat of a long wavelength electromagnetic wave of
frequency $\omega = \omega_p(0)$ and amplitude E_1 , with a static distortion of the

density profile having the form $\delta n = \tilde{n} \exp(ik_0 z)$, the equivalent value of E_0

$$E_0 = \frac{\tilde{n}}{n_0(0)} E_1 . \tag{19}$$

The magnitude of the scaled wave spectrum generated by beat excitation in the direction of decreasing density ($k_0 > 0$) is illustrated in Fig. 5. This figure shows the dependence of $|\tilde{E}(k)|$ on both scaled wave number k/k_A (dashed curve) and on scaled resonant velocity v/v_t (solid curve) for $k_0/k_A = 3$, $\Gamma' = 0.25$, $\alpha = 10$, $k_t/k_A = 6$. In this case the fastest phase velocity present in the spectrum is ω/k_0 (i.e., that of the beat source) since as the wave propagates down the density gradient the WKB wave number increases as $k(z) \sim \sqrt{z}$. A consequence of this dependence is that the modifications in the distribution function are localized in velocity space because no velocities larger than ω/k_0 are present and as in the $k_0 = 0$ case the spectrum is quenched for large k (slower velocities) by Landau damping. In comparing Fig. 5 with Fig. 2, it should be noted that Fig. 2 corresponds to a collisionally dominated plasma in which $\Gamma' = 4$.

The spatial dependence of the electric field modulus $|E|/(k_A L E_0)$ associated with the spectrum of Fig. 5 is displayed in Fig. 6, with the corresponding real part also shown. In comparing Fig. 6 with Fig. 4 it is evident that beat excitation down the density gradient causes a peak enhancement in the resonantly excited wave which is about a factor of 3 smaller than that produced by a $k_0 = 0$ exciter having equal value of E_0. This reduction has two different physical origins: one is a larger group velocity at the resonance location, and the other is larger Landau damping. The resonance location in this case occurs away from the cold plasma resonance layer (i.e., $\omega_p(o) = \omega$) because the beat exciter attains resonance in the neighborhood of

the point where the WKB wave number $k(z)$ of the finite temperature Langmuir wave matches the beat k_O, which for the present case corresponds to $\zeta = 9$, as indicated by the dashed vertical line in Fig. 6. As is seen from this figure, the peak amplitude is shifted down the gradient from the resonance point, a feature which is also present in the $k_O = 0$ case.

The scaled magnitude of the spectrum excited by a beat source propagating in the direction of increasing density ($k_O < 0$) is shown in Fig. 7. The parameters used are the same as those of Fig. 5, except for the sign of k_O, i.e., now $k_O/k_A = -3$. It is seen from Fig. 7 that for this excitation scheme it is possible to cause modifications in the distribution function of particles moving up ($v < 0$) as well as down ($v > 0$) the density gradient because the resonantly excited wave, initially propagating up the gradient, is reflected at the cut-off point at $z = 0$, and proceeds to propagate down the density gradient in a manner similar to that resulting from a $k_O = 0$ exciter.

The spatial dependence of the scaled electric field corresponding to the spectrum of Fig. 7 is displayed in Fig. 8, and is to be compared with the behavior shown in Fig. 6.

III. Modification of Tail Distribution

We proceed to calculate the modification produced in the pre-existing, spatially uniform, fast tail electron distribution by the various self-consistent fields investigated in Sec. II. The quantity of interest here is the time-averaged, spatially asymptotic change in the distribution function, accurate to second order in E_0. The meaning of the time average refers to time samples long compared to the period of the coherent oscillation, i.e., $\Delta t \gg 2\pi/\omega_0$. Spatially asymptotic implies that the region of interest is far from the spatial point where the wave particle resonance is encountered for a given velocity, i.e., where $k(z) = \omega/v$. The restriction to second order perturbation theory implies that strong nonlinear wave-particle interactions, such as particle trapping, are not included.

It is useful to express the time-averaged tail distribution function in the form

$$< f_t^{\pm} \ (z = \pm\infty, v) \ > \ = \ f_{ot}(v) \ + \ < \ \delta f_t^{\pm} \ (z = \pm\infty, v) \ > \ , \qquad (20)$$

where the $\pm$ label refers to $v > 0$ and $v < 0$ particles, respectively, and the $<>$ represents the time-averaging operation.

The modification in the distribution function is obtained by integrating the time-averaged Vlasov equation in configuration space using appropriate boundary conditions for $v > 0$ and $v < 0$, namely $<\delta f_t^{+} \ (z = -\infty, v)> \ = \ <\delta f_t^{-} \ (z = \infty, v)> \ = \ 0.$ The relevant expression for $v > 0$ is

$$< \delta f_t^{+} \ (z = \infty, v)> \ = \ \frac{e}{4mv} \ \frac{\partial}{\partial v} \ \{ \int_{-\infty}^{\infty} dz' E(z') \ [f_1^{+} \ (z', v)]^* \ \} \ + \ c.c. \ , \qquad (21)$$

where, $f_1^{+} \ (z', v)$ is the first order modified distribution function oscillating as $\exp(-i\omega t)$ and given by

$$f_1^+ (z',v) = \frac{e}{mv} \frac{\partial}{\partial v} f_{ot}(v) \int_{-\infty}^{z'} dz'' \exp\left[i \frac{\omega}{v} (z'-z'')\right] E(z'') . \qquad (22)$$

Inserting Eq. (22) into Eq. (21) and representing the spatially dependent electric fields in terms of the Fourier transform defined by Eq. (15) yields the familiar expression

$$\langle \delta f_t^+ (z=-\infty,v) \rangle = \left(\frac{e}{2m}\right)^2 \frac{1}{v} \frac{\partial}{\partial v} \left\{ \left| \tilde{E}\left(k = \frac{\omega}{v}\right) \right|^2 \frac{1}{v} \frac{\partial}{\partial v} f_{ot} \right\}, \qquad (23)$$

in which it has been consistently assumed in all intermediate integrations that ω has an infinitesimally small imaginary part that causes the oscillatory contribution at $z = -\infty$ to vanish. A similar procedure using the appropriate boundary conditions for $v < 0$ particles yields an identical expression, thus permitting the generalization

$$\langle \delta f_t^\pm (z=\pm\infty,v) \rangle = \left(\frac{e}{2m}\right)^2 \frac{1}{v} \frac{\partial}{\partial v} \left\{ \left| \tilde{E}\left(k = \frac{\omega}{v}\right) \right|^2 \frac{1}{v} \frac{\partial}{\partial v} f_{ot} \right\}. \qquad (24)$$

It should be mentioned that the expression in Eq. (24) is often referred to as the quasilinear result, but in the present context it should be properly interpreted as the spatially asymptotic, second order, time-averaged modification produced by a temporally coherent exciter.

A. **Uniform Pump**

The spectrum excited by a $k_o = 0$ source in a nonuniform plasma is strictly unidirectional, as shown in Eqs. (13) and (14). Consequently, the modifications in the tail distribution function are restricted to those particles that propagate in the direction of decreasing density, which implies that $\langle \delta f^- \rangle = 0$ or

$$\langle f_t^- (z=-\infty,v) \rangle = f_{ot}(v) \quad , \qquad (25)$$

and

$$\langle f_t^+(z=\infty,v)\rangle = f_{ot}(v) \left[1 + \left(\frac{E_0}{E_s}\right)^2 h^+(v)\right] \quad , \tag{26}$$

where

$$h^+(v) = \{1-2[\frac{v_t^2 v_L}{v^3} + \alpha \exp(-v^2/2v_t^2)]\} \times$$

$$\exp\{-2[\frac{v_L}{v} + \alpha \exp(-v^2/2v_t^2)]\} \quad , \tag{27}$$

and in which the quantity $E_s \equiv mv_t^2/(e\pi L)$ represents the natural scaling for the strength of the pump field E_0 that can cause significant tail modifications. In the manipulations leading to Eqs. (26) and (27) the explicit form of $f_{ot}(v)$ given by Eq. (6) has been used and we note that $v_L = \Gamma\omega L = \omega/k_L$.

It should be emphasized that Eqs. (26) and (27) apply to both extreme limits of resonant exicitation by a $k_0 = 0$ pump, i.e., to the Lorentzian and to the driven Airy pattern. In spite of the important role played by the characteristic wave number k_A in determining the spatial pattern seen in the curves of Fig. 4, it plays no role in Eqs. (26) and (27), i.e., the modifications in the distribution function are independent of k_t/k_A . The relevant scaled parameters that determine second order modifications of the tail distribution by a $k_0 = 0$ exciter are: E_0/E_s, v_L/v_t, and α.

In the large velocity limit, i.e., $v \gg v_L$ and $v \gg \sqrt{2}\,\bar{v}_t$,

$$\langle f_t^+(z=\infty,v)\rangle \rightarrow f_{ot}(v) \left[1 + \left(\frac{E_0}{E_s}\right)^2\right] \quad , \tag{28}$$

which implies an enhancement of the density of extremely energetic electrons with no change in the shape of their velocity distribution. This behavior occurs because the derivative of the modulus of the spectrum with respect to velocity goes to zero at large velocities and the velocity derivative of a Maxwellian tail distribution goes as $\partial f_{ot}/\partial v \rightarrow -v f_{ot}/v_t^2$ so that the spatially

asymptotic, time-averaged change has the form

$$\langle \delta f_t^+ (z{=}\infty,v)\rangle \rightarrow \frac{1}{v}\frac{\partial}{\partial v}\left[\frac{D}{v}\frac{\partial f_{ot}}{\partial v}\right] \quad , \tag{29}$$

with $D \equiv (e/2m)^2\,|\tilde{E}(k{=}\omega/v)|^2$ nearly constant, hence

$$\langle \delta f_t^+ (z{=}\infty,v)\rangle \rightarrow \frac{D}{v_t^{\;4}}\,f_{ot}(v) \quad , \tag{30}$$

which indicates an energetic tail density enhancement of $n_t\,D/v_t^{\;4}$, independent of v_L and α .

Figure 9 illustrates various properties of the second order modifications produced by a $k_o = 0$ exciter; it displays logarithmic plots of the spatially asymptotic, time-averaged distribution function versus scaled velocity $v/\sqrt{2}\,v_t$ for different conditions. The curve labelled $E_o = 0$ is the zero order tail distribution and the solid curve marked $\alpha = 0$ provides an example of a non-self-consistent calculation (spectrum determined entirely by collisions) for $v_L/\sqrt{2}\,v_t = 3$, $(E_o/E_s)^2 = 35$. The dashed curve is a self-consistent result for a scaled tail density $\alpha = 30$. It is seen from Fig. 9 that for large velocities the self-consistent and non-self-consistent results are identical and cause a direct enhancement in the energetic tail density, as explained by Eq. (30). The modification produced by the non-self-consistent spectrum is gentler in slope and extends to lower velocities than that caused by the self-consistent spectrum, as anticipated from the behavior displayed in Fig. 2. The increased value of $\partial|\tilde{E}(k{=}\omega/v)|^2/\partial v$ due to self-consistent depletion of the large k components of the spectrum by Landau damping gives rise to a strong modification of the velocity distribution over a narrow velocity interval. In particular, as the value of the parameter α is increased, for fixed E_o/E_s, it is possible for the tail distribution to develop a positive

slope over a restricted velocity range, as is illustrated in Fig. 10 for $(E_o/E_s)^2 = 60$, $v_L/\sqrt{2}\, v_t = 3$. It is seen from Fig. 10 that the non-self-consistent calculation (solid curve labelled $\alpha = 0$) predicts a monotonic distribution function, while the self-consistent analysis yields a bump-on-tail distortion for $\alpha = 50$. For reference, the unperturbed distribution is indicated by the dashed curve ($E_o = 0$).

Since the requirements for slope reversal with a $k_o = 0$ exciter have been discussed in our earlier[1] non-self-consistent study in which the modulus of the spectrum is determined entirely by collisions, we want to emphasize that, for a self-consistent field in a collisionless plasma slope reversal can also result within second order theory, as is illustrated in Fig. 11 for $\Gamma = 0$, $\alpha = 10$, and a relatively small pump amplitude $E_o/E_s = \sqrt{5}$.

The threshold condition on the pump amplitude E_o required to develop slope reversal is obtained in the general case by setting

$$\frac{\partial}{\partial v} \langle f_t^+ (z=\infty, v)\rangle = 0 \quad , \tag{31}$$

and using Eq. (26) to solve for $(E_o/E_s)^2$

$$\left(\frac{E_o}{E_s}\right)^2 = \frac{v}{v_t{}^2} \left[\frac{\partial}{\partial v} h^+(v) - \frac{v}{v_t{}^2} h^+(v)\right]^{-1} \quad , \tag{32}$$

which using Eq. (27) takes the form

$$\left(\frac{E_o}{E_s}\right)^2 = b^{-1} \exp\left[(2v_L/v_t) + 2\alpha \exp(-v^2/2v_t{}^2)\right] \quad , \tag{33}$$

where

$$b = (6v_t{}^4 v_L/v^5) + 2\alpha \exp(-v^2/2v_t{}^2) -$$

$$\left[1 - (2v_t{}^2 v_L/v^3) - 2\alpha \exp(-v^2/2v_t{}^2)\right]^2 \quad . \tag{34}$$

Since the left-hand side as well as the right-hand exponential factor in Eq. (33) are positive definite, it follows that slope reversal within second order perturbation theory can occur only for that restricted velocity interval in the distribution function over which the quantity b given by Eq. (34) is positive. In general this range in v depends on the parameters v_L/v_t and α through a transcendental equation that must be solved numerically. However, in the non-self-consistent limit ($\alpha = 0$), the range satisfies the inequality

$$\frac{2v_L}{v} - \left(\frac{6v_L}{v}\right)^{1/2} < \left(\frac{v}{v_t}\right)^2 < \frac{2v_L}{v} + \left(\frac{6v_L}{v}\right)^{1/2} \quad , \tag{35}$$

while in the collisionless limit ($v_L = 0$) b is positive in the range,

$$\ln\left[4\alpha/(3 + \sqrt{5})\right] < \left(\frac{v}{\sqrt{2}\,v_t}\right)^2 < \ln\left[4\alpha/(3 - \sqrt{5})\right] \quad . \tag{36}$$

Because the inequality of Eq. (36) exhibits a logarithmic dependence on α the range over which slope reversal can develop in the collisionless limit is narrower than in the non-self-consistent ($\alpha = 0$) limit. Thus a threshold field exists for producing slope reversal but only over a limited range in velocity space.

B. Beat Excitation

For a beat source having $k_0 > 0$ the resulting electric field spectrum given by Eq. (12) is unidirectional, as is the case for a $k_0 = 0$ exciter, but the fastest Fourier component present has phase velocity $v_0 = \omega/k_0$. Consequently, the modifications in the fast electron distribution function

caused by this excitation process are restricted to electrons moving in the direction of decreasing density within the interval $0 < v < v_0$, i.e.,

$$\langle f_t^- (z=-\infty,v)\rangle = f_{ot}(v) \quad , \tag{39}$$

and

$$\langle f_t^+ (z=\infty,v)\rangle = f_{ot}(v) \left[1 + \left(\frac{E+}{E_s}\right)^2 h^+(v)\theta(v_0 - v)\right] \quad , \tag{40}$$

where $h^+(v)$ is given by Eq.(28), θ is the Heaviside step function, and now from Eq. (12) the factor $\exp[-F(k_0)]$ enters and the role of the pump strength E_0 in the $k_0 = 0$ case is replaced by

$$E_+ = E_0 \exp\left[\frac{v_L}{v_0} + \alpha \exp\left(-v_0^2/2v_t^2\right)\right] \quad . \tag{41}$$

A significant difference from the effect caused by a $k_0 = 0$ pump is that the enhancement in the density of extremely energetic electrons, given by Eq. (28), is not present. In addition, the formation of a positive slope in the distribution function requires the phase velocity of the beat source to be larger than the smallest velocity for which the factor b of Eq. (34) vanishes, e.g., in the collisionless limit it requires that

$$\left(\frac{v_0}{\sqrt{2} \, v_t}\right)^2 > \ln\left[4\alpha/(3+\sqrt{5})\right] \quad . \tag{42}$$

For beat sources satisfying this condition the threshold electric field for bump formation is given by the expression in Eq. (33), but with E_0 replaced by E_+. The characteristic features of modifications produced by a $k_0 > 0$ beat source are summarized in Fig. 12 for $v_0/\sqrt{2} \, v_t = 3.5$, $v_L/\sqrt{2} \, v_t = 4$, $\alpha = 10$, and $(E_0/E_s)^2 = 30$.

A beat source having $k_0 < 0$ gives rise to a bi-directional electric field spectrum, but its effect on the tail distribution function is asymmetric

with respect to particles moving up or down the density profile. For particles with $v > 0$ the modification is similar to that caused by a $k_o = 0$ exciter, i.e.,

$$\langle f_t^+ (z=\infty,v)\rangle = f_{ot}(v)\left[1 + \left(\frac{E_-}{E_s}\right)^2 h^+(v)\right] \quad , \tag{41}$$

with the pump strength E_o now replaced by

$$E_- = E_o \exp\left[-\frac{v_L}{|v_o|} + \alpha \exp\left(-v_o^2/2v_t^2\right)\right] \quad . \tag{42}$$

For $v < 0$ particles the modification is restricted to velocities having magnitude larger than $|v_o|$, because the resonantly excited wave initially having phase velocity $-\omega/|k_o| = v_o$ approaches cut-off and the phase velocity increases, i.e, in the WKB sense $\omega/k(z) \to -\infty$ as $z \to 0^+$. The modified distribution function in the range $v < 0$ is

$$\langle f_t^- (z=-\infty,v)\rangle = f_{ot}(v)\left[1 + \left(\frac{E_-}{E_s}\right)^2 h^+(v)\theta(|v| - |v_o|)\right] \quad . \tag{43}$$

In this excitation scheme there is an identical energetic electron density enhancement $n_t\left[1 + (E_-/E_s)^2\right]$ produced up and down the density profile. For $v > 0$ particles the condition for bump formation is similar to that of the $k_o = 0$ pump except for the replacement of E_o by E_- in Eq.(33). An example of a distribution modified by a $k_o < 0$ exciter is given in Fig. 13 for $v_o/\sqrt{2}\,v_t = -3$, $v_L/\sqrt{2}\,v_t = 10^{-3}$, $\alpha = 10$, $(E_o/E_s)^2 = \sqrt{6}$. Note that in Fig. 13 the distribution functions $\langle f_t^\pm\rangle$ are presented for illustrative purposes as a single function of velocity, but it should be understood that the domain $v < 0$ is found spatially at $z \to -\infty$, while $v > 0$ corresponds to $z \to \infty$.

IV. Conclusions

An analytic study has been made of the self-consistent modifications produced on a pre-existing fast electron distribution function in a nonuniform plasma which is subjected to resonant excitation by external wave sources. Since the wave-particle interaction analyzed here is restricted to a fast tail distribution which is initially spatially uniform while the nonuniform warm background plasma undergoes collisional heating, the results are applicable to experiments in which the plasma has a long density scale length, i.e., $(k_D L)^{1/3} \gg 1$. Such a parameter ordering is realizable in the laboratory, and is naturally achieved in ionospheric and space plasmas.

Although the time-averaged modification in the distribution function has been determined self-consistently, the calculation has been performed only to second order accuracy in the strength of the electric fields. This implies that strongly nonlinear effects such as particle trapping and nonlinear shifts in the wave-particle resonance condition $v = \omega/k(z)$ are not included.

One of the interesting results of the present analysis is that a positive slope can be formed in the distribution function by self-consistent second order nonlinearities in a nonuniform plasma. The cause of this effect can be traced to the competition between the negative slope of the zero order distribution function $f_{ot}(v)$ and the positive slope of the self-consistent spectrum, i.e., $\partial |\tilde{E}(k=\omega/v)|^2/\partial v > 0$. Physically, these opposing tendencies result in the existence of a restricted velocity interval within which more particles are accelerated out of the interval toward larger velocities than enter into it from lower velocities, provided the pump field amplitude E_0 is above a threshold value. It is found here that self-consistency increases the value of $\partial |\tilde{E}(k=\omega/v)|^2/\partial v$ and hence lowers the threshold for bump forma-

tion from the value predicted by a non-self-consistent analysis. This feature
is worth emphasizing because on first thought one might expect the opposite
behavior, i.e., self-consistency reduces the amplitude of the spectrum and
hence the modifications should be weaker. That is not the case because the
quantity of relevance is the slope of the spectrum, which is found to
increase as the scaled tail density parameter $\sigma = (n_t/n_o)(\pi/2)^{1/2}(\bar{v}/v_t) \, k_D L$
increases.

A significant experimental consequence of slope reversal in the fast tail
distribution function is the spontaneous growth of waves (or sidebands) having
frequencies different from that of the monochromatic external signal driving
the linear plasma resonance. It is important to assess the role of such an
effect when interpreting experimental observations of extraneous frequencies
in resonant absorption experiments in plasmas since its presence can be
confused with parametric instabilities. While in numerous cases parametric
instabilities are indeed present, it is possible that some of the observed
spectral features actually arise from wave induced distortions in the distrib-
ution function. As suggested by the present study this is a topic that
deserves closer scrutiny in the context of specific experiments. In fact,
experiments[19,20] performed in uniform plasmas excited with grid antennas have
been found to exhibit an analogous effect.

In the study of the self-consistent resonant electric fields two possible
excitation models have been considered which describe a broad class of
experimentally interesting scenarios. For instance, the $k_o = 0$ exciter can
model the irradiation of an unmagnetized plasma with an electromagnetic wave
propagating obliquely to the density gradient. This same model also describes
the fields produced during mode conversion of an oblique electrostatic
whistler into a Langmuir wave in a magnetized plasma. The other excitation

mechanisms considered ($k_0 > 0$, $k_0 < 0$) model sources which experimentally can arise from the beat of two transparent electromagnetic waves, as is presently being considered in the context of laser accelerators, or may result from the beat of an external electromagnetic wave with low frequency distortions of the density profile. For completeness, in the present work we have also indicated how the effective pump strength E_0 is related to the various physical parameters for these different resonant excitation schemes.

Beat sources that propagate in the direction of decreasing density with velocity $v_0 > 0$ are found to cause distortions in the tail distribution within the interval $v_0 > v > 0$ because the WKB phase velocity of the resonantly excited wave decreases as it propagates down the density gradient. Although it is possible to obtain second order slope reversal in this scheme, the possibility is restricted by the value of v_0. The effect of a beat source propagating in the direction of increasing density $v_0 < 0$ is highly nonlocal. For $z \rightarrow -\infty$ it causes a modification in the distribution function for fast particles satisfying $v < v_0 < 0$, while simultaneously modifying the distribution function over the entire velocity range at $z \rightarrow \infty$.

In summary, various features of self-consistent wave-particle inter-actions in nonuniform plasmas have been ellucidated by this analytic study. It is hoped that some of the results will help in the interpretation of laboratory and ionospheric experiments and stimulate more advanced analysis of kinetic processes in nonuniform media.

Acknowledgements

The authors are especially indebted to Ms. Aileen Wang for numerical computations relating to this work. Valuable insight was also provided from integral equation solutions of resonant excitation obtained by Prof. B. D. Fried.

Bibliography

1. M.M. Shoucri, G.J. Morales, and J.E. Maggs, J. Geophys. Res. 92, 246 (1987).

2. J.E. Maggs, G.J. Morales, and A. Baños, APS Bull. 30, 1562 (1985).

3. For a general overview of recent developments consult Laser Acceleration of Particles, AIP Conf. Proc. No. 130, C. Joshi and T. Katsouleas, eds. (AIP, New York, 1985).

4. A.Y. Wong, G.J. Morales, D. Eggleston, J. Santoru, and R. Behnke, Phys. Rev. Lett. 47, 1340 (1981).

5. G.J. Morales, A.Y. Wong, J. Santoru, L. Wang, and L. Duncan, Radio Science 17, 1313 (1982).

6. For a partial account of recent literature consult Phys. Fluids Commulative Index, Vols. 24-28 (1981-1985), p. 73.

7. W.M. Manheimer and H.H. Klein, Phys. Fluids 18, 1299 (1975).

8. J. Albritton and P. Koch, Phys. Fluids 18, 1136 (1975).

9. D.W. Forslund, J.M. Kindel, and K. Lee, Phys. Rev. Lett. 39, 284 (1977).

10. K.G. Estabrook and W.L. Kruer, Phys. Rev. Lett. 40, 42 (1978).

11. B. Bezzerides and S.J. Gitomer, Phys. Rev. Lett. 46, 593 (1981).

12. A. Simon, W. Seka, L.M. Goldman, and R.W. Short, Phys. Fluids 29, 1704 (1986).

13. M. Colunga, J.F. Luciani, and P. Mora, Phys. Fluids 29, 3407 (1986).

14. G.J. Morales and Y.C. Lee, Phys. Fluids 20, 1135 (1977).

15. H.A. Antosiewicz, in Handbook of Mathematical Functions, edited by M. Abromowitz and I.A Stegun (Dover, New York, 1970), p. 446.

16. D.K. Kelly and A. Baños, University of California, Los Angeles Plasma Physics Group Report PPG-170 (1974).

17. D.W. Forslund, J.M. Kindel, K. Lee, E.L. Lindman, and R.L. Morse, Phys. Rev. A 11, 679 (1975).

18. T. Speziale and P.J. Catto, Phys. Fluids 20, 990 (1977).

19. T.P. Starke and J.H. Malmberg, Phys. Fluids 21, 2242 (1978).

20. E. Märk, R. Hatakeyama, and N. Sato, Plasma Phys. 20, 415 (1978).

Figure Captions

Fig. 1   Schematic of geometry considered. The background density profile $n_0(z)$ is approximately linear near the plasma resonance located at $z = 0$, while the fast electron density profile n_t is uniform. The characteristic velocity of tail electrons scales as $v_t \sim (k_D L)^{1/3} \, \bar{v}$ and the various excitation scenarios are modelled by $S(z)$.

Fig. 2   Modulus of spectrum excited by $k_0 = 0$ source. Dashed curves show wave number dependence (top scale) and solid curves resonant velocity dependence (bottom scale). $\alpha = 0$ corresponds to collisional damping alone, and finite α indicates effect of self-consistency for $k_L/k_A = 0.25$, $k_t/k_A = 6$.

Fig. 3   Spatial dependence of scaled modulus of collisionally limited resonant electric field excited by $k_0 = 0$ source. Solid curve shows dependence in the absence of fast electrons and dashed curve exhibits the self-consistent effect of tail Landau damping for a scaled tail density $\alpha = 10$ and $k_t/k_L = \sqrt{3}$. $k_L \equiv (\omega/v)L^{-1}$ and α is defined after Eq. (14).

Fig. 4   Spatial dependence of scaled modulus of electric field for a convectively limited resonance. Top curve is the undamped mode conversion result $\pi |Gi(-\zeta) + i \, Ai(-\zeta)|$, and the curve $\Gamma' = 0.25$, $\alpha = 10$ shows the effect of collisions. The bottom curve contains collisional and fast electron tail Landau damping for $\Gamma' = 0.25$, $\alpha = 10$, and $(k_t/k_A)^2 = 40$. $k_A \equiv (k_D L/\sqrt{3})^{2/3} L^{-1}$, and α is the scaled tail density defined after Eq. (14).

Fig. 5   Modulus of spectrum excited by a beat source propagating in the direction of decreasing density with $k_o/k_A = 3$. Dashed curve (top scale) shows dependence on scaled wave number and solid curve (bottom scale) the resonant velocity dependence $k = \omega/v$ for $\Gamma' = 0.25$, $\alpha = 10$, $k_t/k_A = 6$.

Fig. 6   Spatial dependence of scaled modulus and real part of electric field excited by a beat source propagating in the direction of decreasing density with $k_o/k_A = 3$ and corresponding to the spectrum shown in Fig. 5. The dashed vertical line indicates the WKB wave resonance point, i.e., where $k(z) = k_o$.

Fig. 7   Scaled magnitude of spectrum excited by a beat source propagating in the direction of increasing density, $k_o/k_A = -3$, $\Gamma' = 0.25$, $k_T/k_A = 6$, $\alpha = 10$. Dashed curve (top scale) is the wave number dependence and solid curve (bottom scale) the resonant velocity dependence $k = \omega/v$.

Fig. 8   Spatial dependence of scaled modulus and real part (dashed curve) of electric field excited by a beat source propagating in the direction of increasing density with $k_o/k_A = -3$ and corresponding to the spectrum shown in Fig. 7. The dashed vertical line indicates the WKB wave resonance point, i.e., where $k(z) = k_o$.

Fig. 9   Distortion in tail velocity distribution function caused by a $k_o = 0$ exciter. The curve labelled $E_o = 0$ is the zero order distribution, while the $\alpha = 0$ gives the non-self-consistent result. The dashed curve is a self-consistent calculation for $\alpha = 30$, $v_L/\sqrt{2}\, v_t = 3$, $(E_o/E_s)^2 = 35$.

Fig. 10   Example of localized distortion of distribution function caused by self-consistency. Dashed curve is zero order distribution, curve labelled $\alpha = 0$ is non-self-consistent result for $v_L/\sqrt{2}\, v_t = 3$, $(E_0/E_s)^2 = 60$, and curve labelled $\alpha = 50$ is self-consistent calculation.

Fig. 11   Example of collisionless ($\Gamma = 0$) slope reversal caused by relatively small pump field $E_0/E_s = \sqrt{5}$. Dashed curve is the zero order tail distribution and solid curve the modified distribution for a scaled tail density $\alpha = 10$.

Fig. 12   Modification of the tail distribution function produced by a beat source propagating in the direction of decreasing density with $v_0/\sqrt{2}\, v_t = 3.5$ for $v_L/\sqrt{2}\, v_t = 4$, $\alpha = 10$, $(E_0/E_s)^2 = 30$. The dashed curve is the zero order distribution.

Fig. 13   Modifications of the tail distribution function produced by a beat source propagating in the direction of increasing density with $v_0/\sqrt{2}\, v_t = -3$ for $\alpha = 10$, $v_L/\sqrt{2}\, v_t = 10^{-3}$, $(E_0/E_s) = \sqrt{6}$. Note that the modifications for $v < 0$ appear as $z \to -\infty$, while those for $v > 0$ correspond to $z \to \infty$. The dashed curve is the zero order tail distribution.

$E_0 S(z) e^{-i\omega t}$

$n_T(z)$

$n_0(z)$

$v_T \sim (k_D L)^{1/3} \bar{v}$
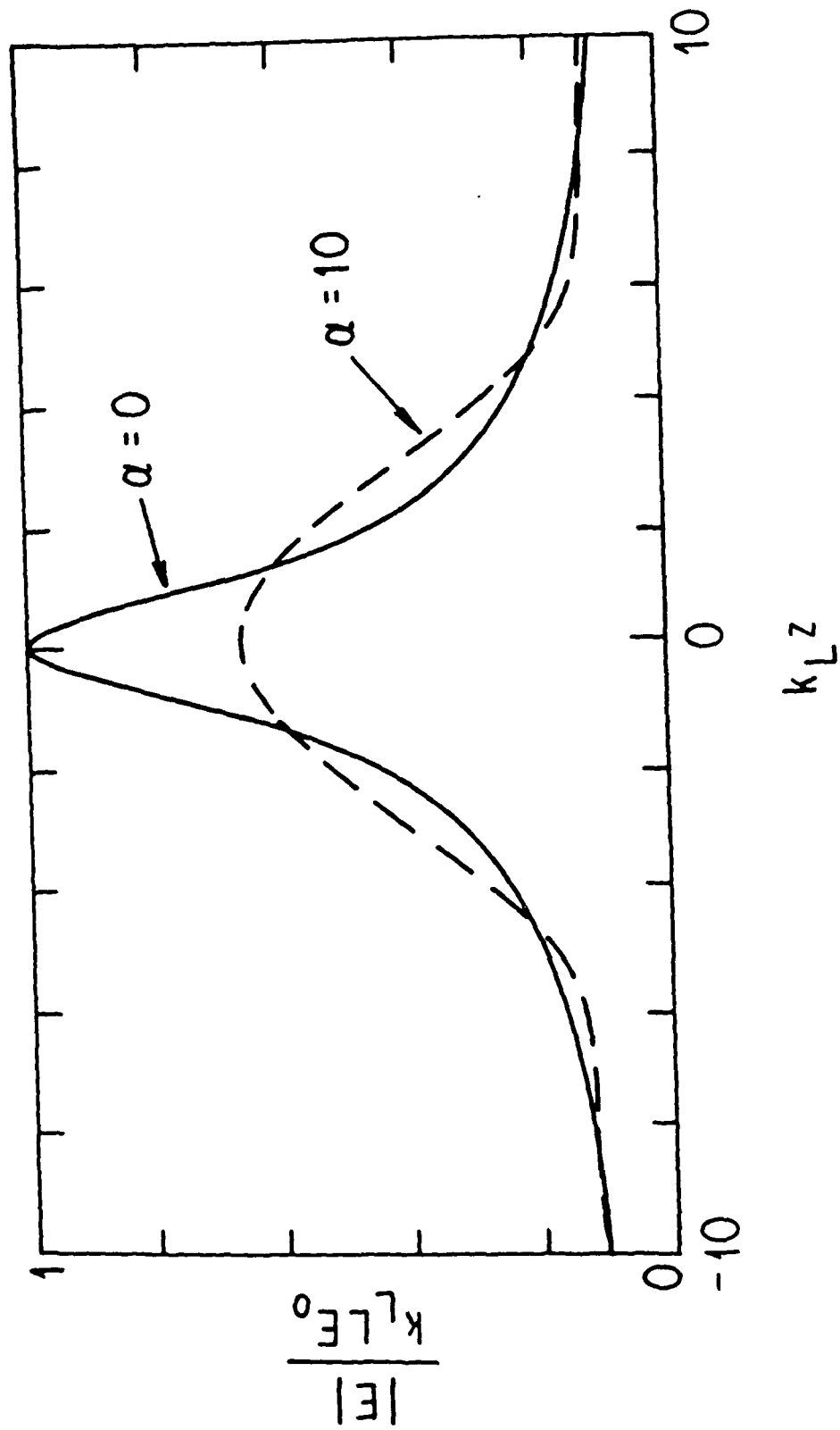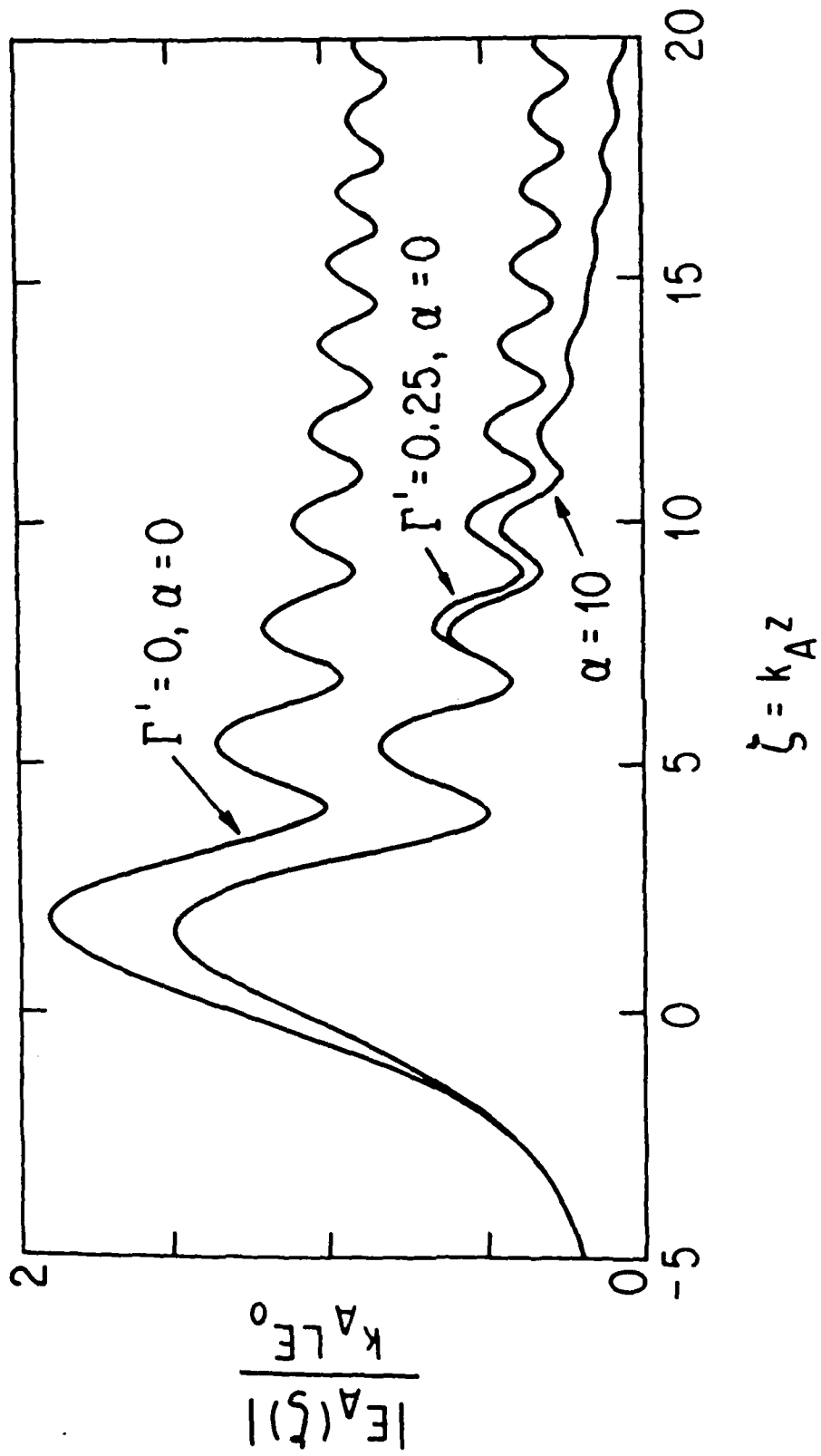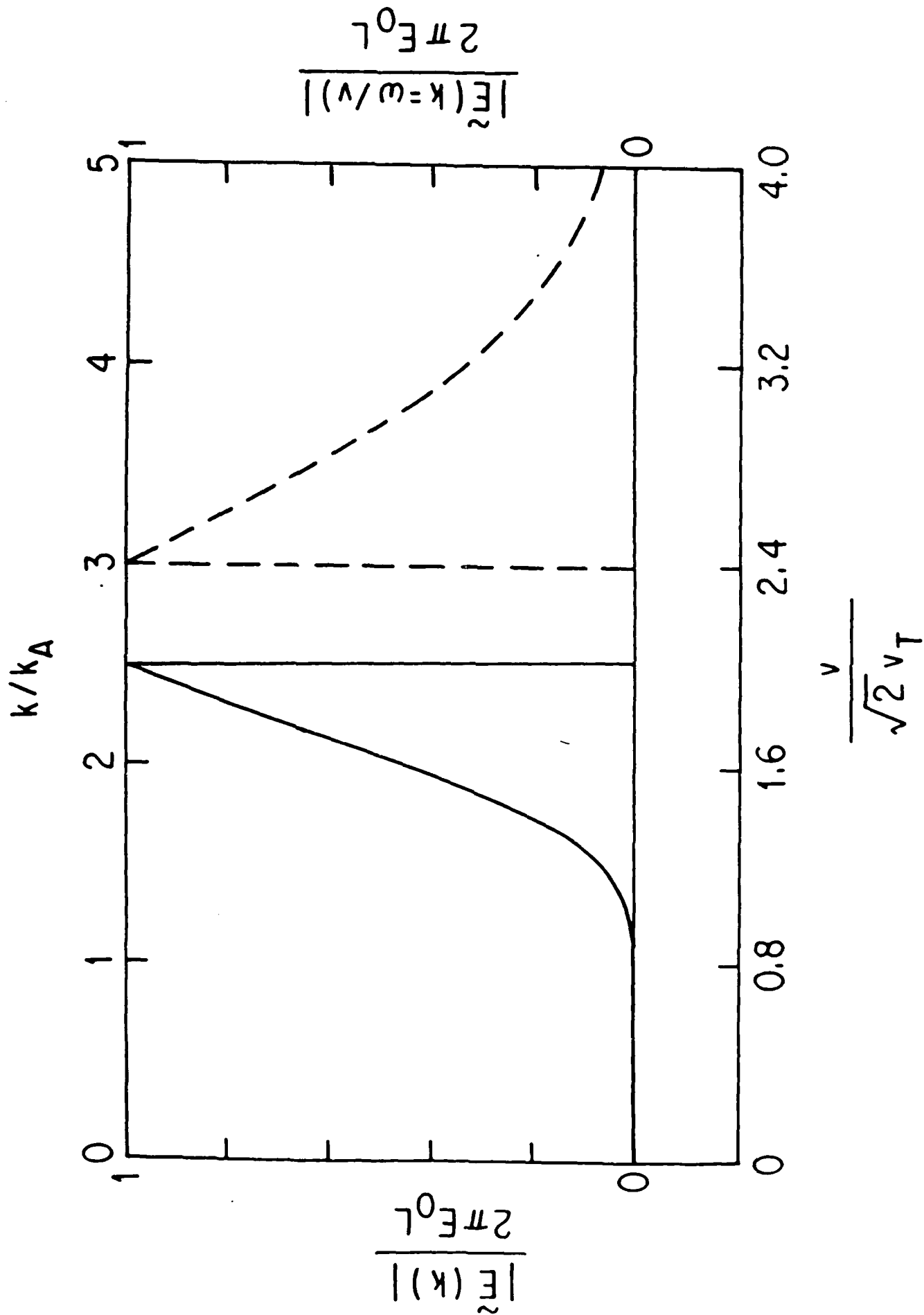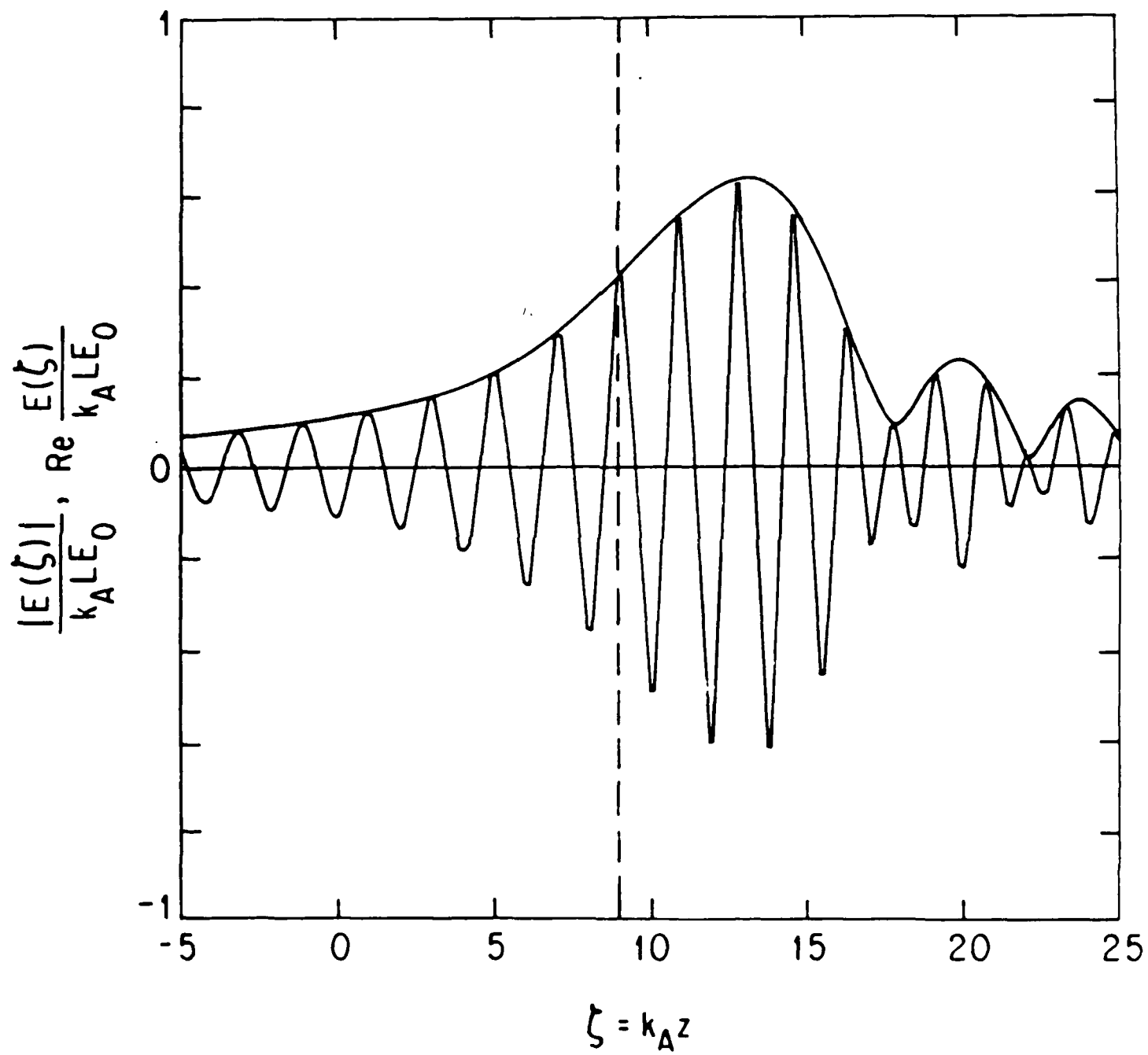
$\omega_p = \omega$
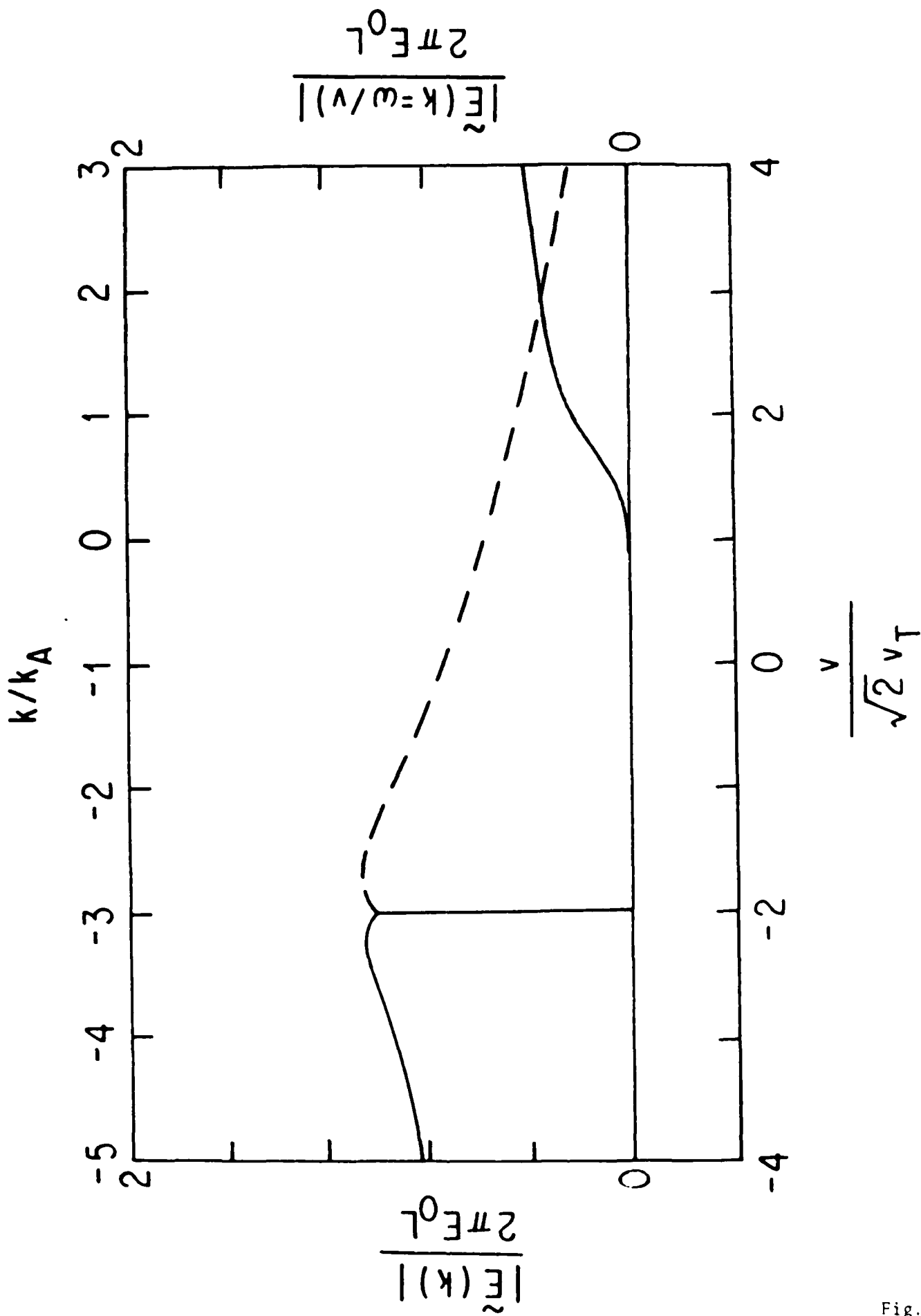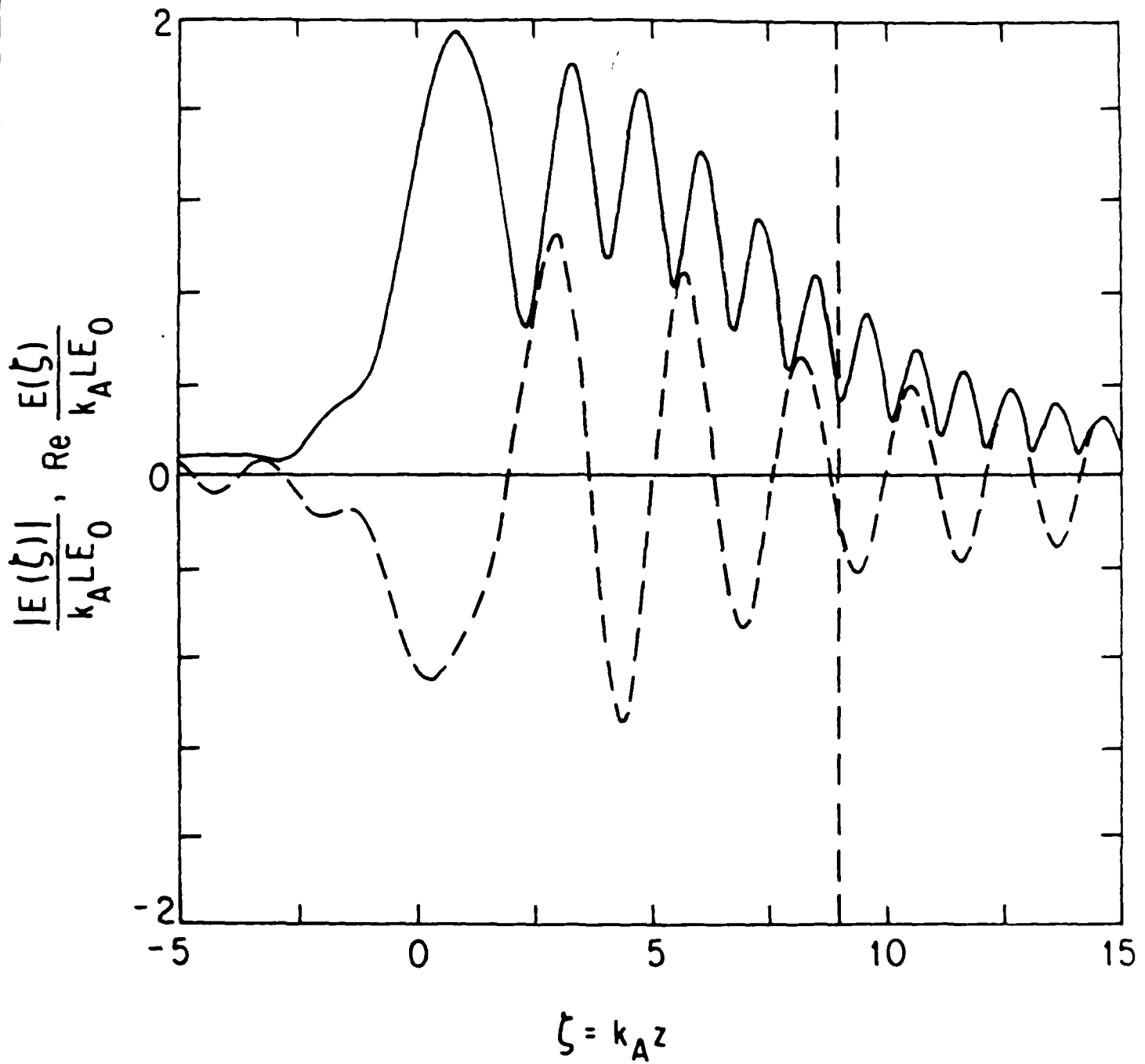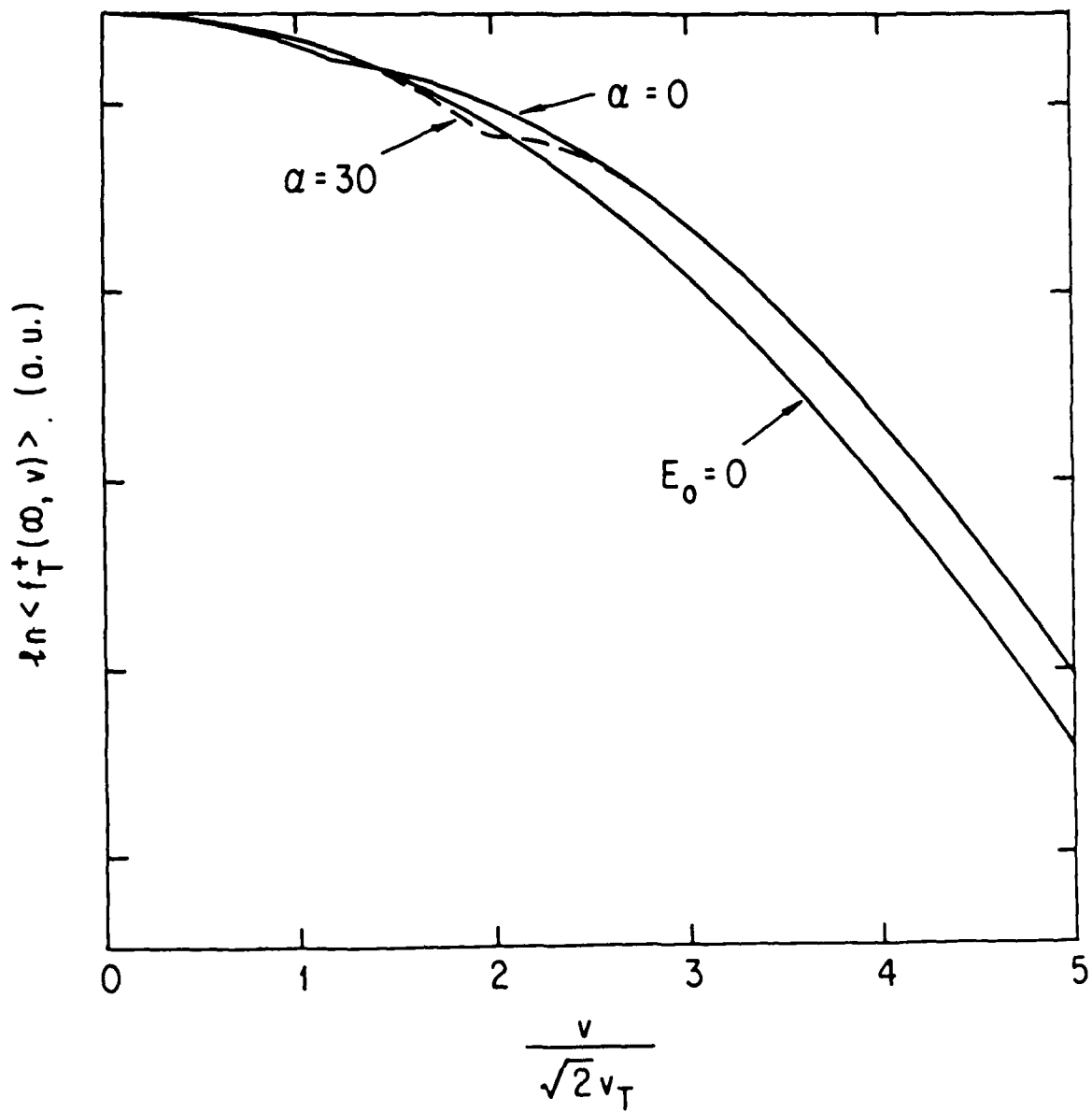
$z = 0$

$+\infty$

$-\infty$
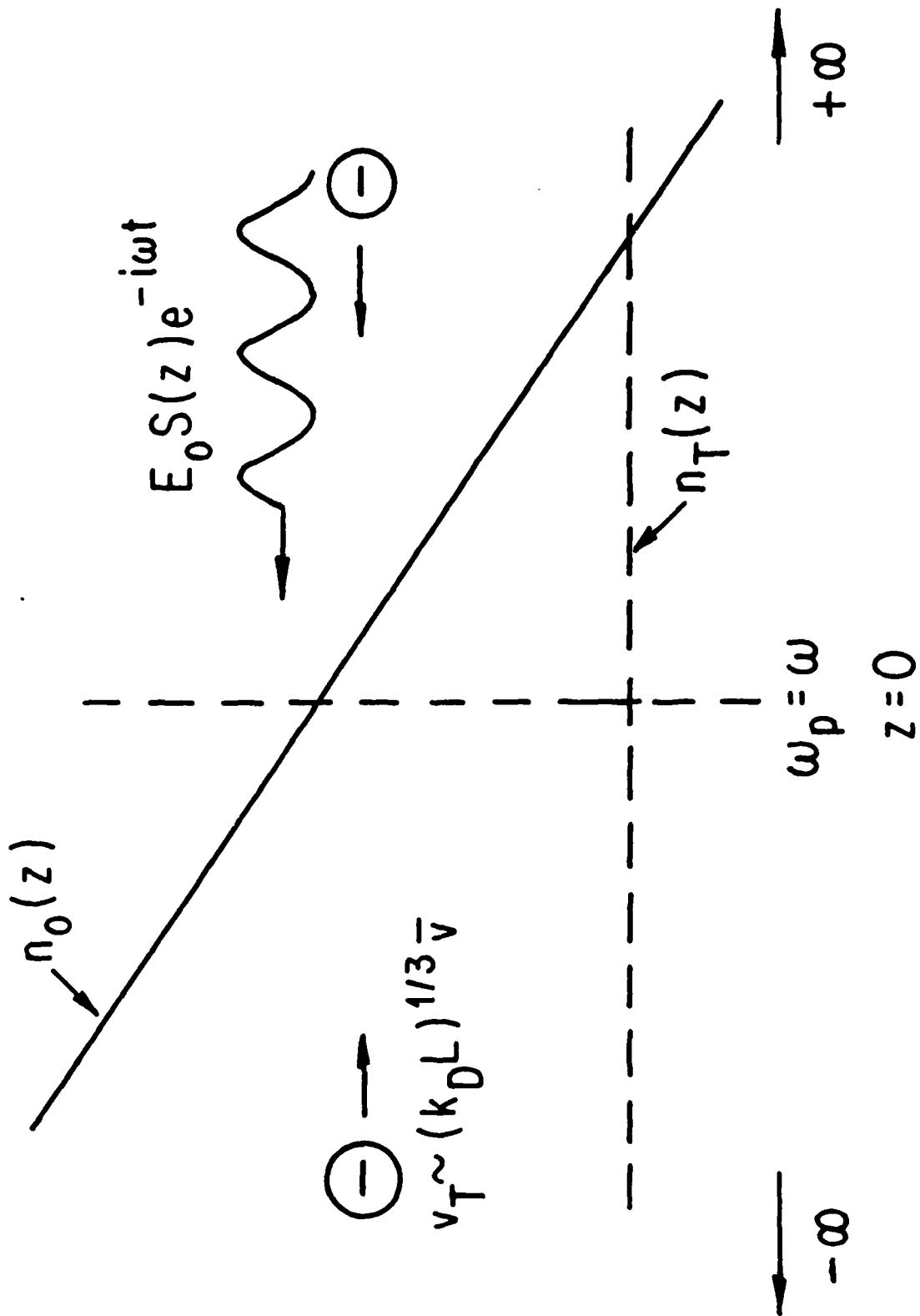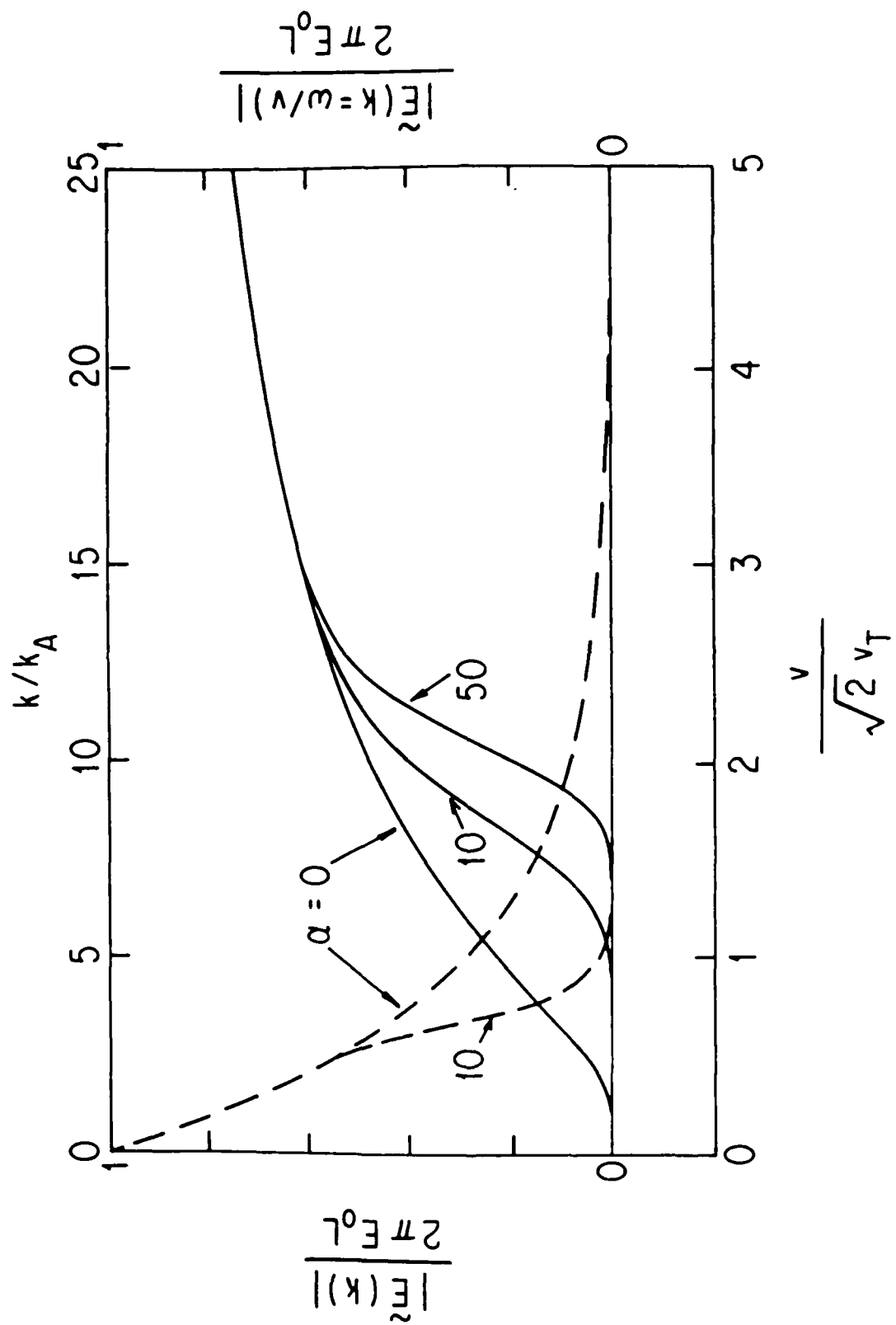
Fig. 1

Fig. 2

Fig. 3

Fig. 4

Fig. 5

Fig. 6

Fig. 7

Fig. 8

Fig. 9

Fig. 10

Fig. 11

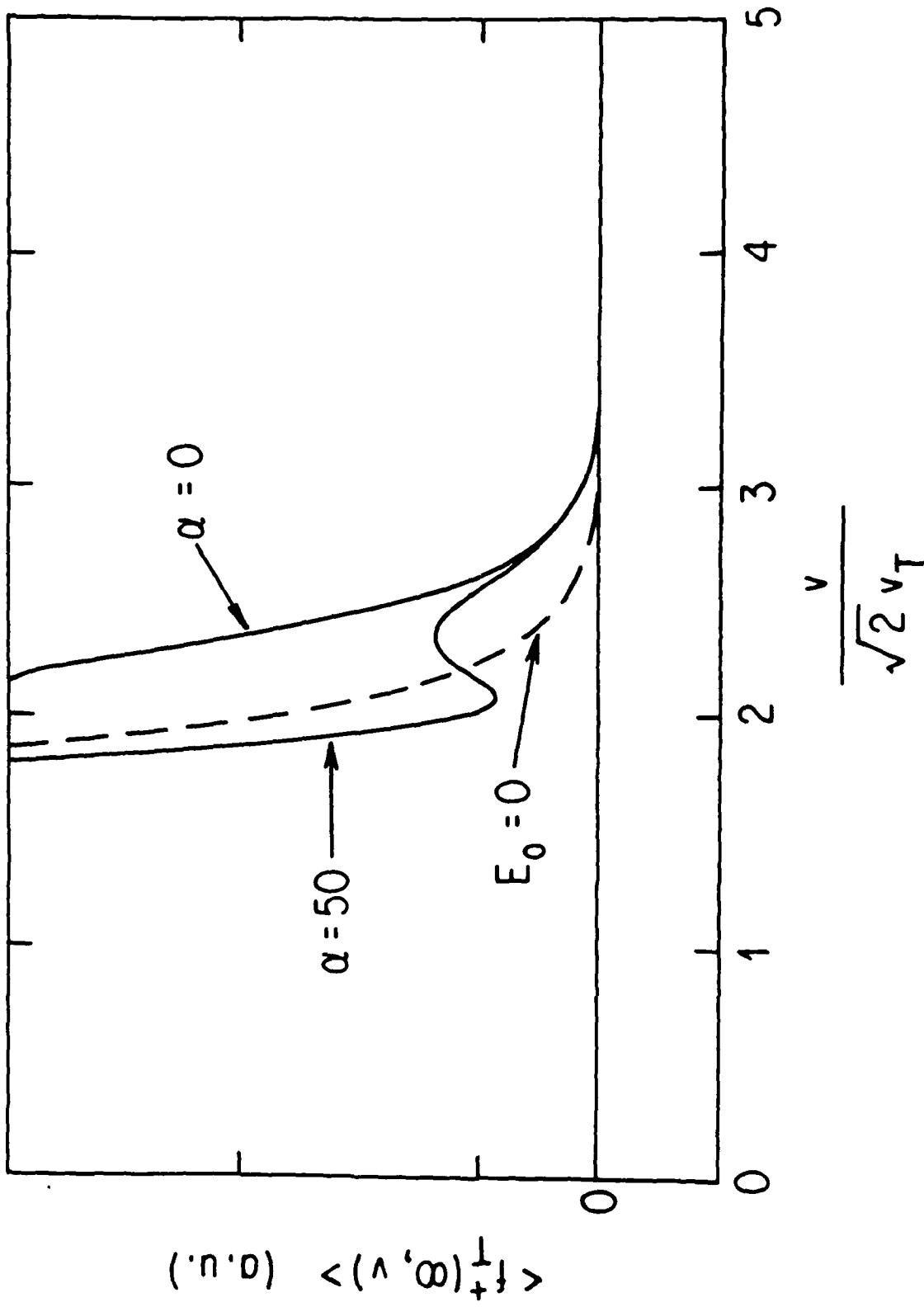$\ell n \langle f_T \rangle$ (a.u.)

$E_0 = 0$

$\dfrac{v}{\sqrt{2}\, v_T}$
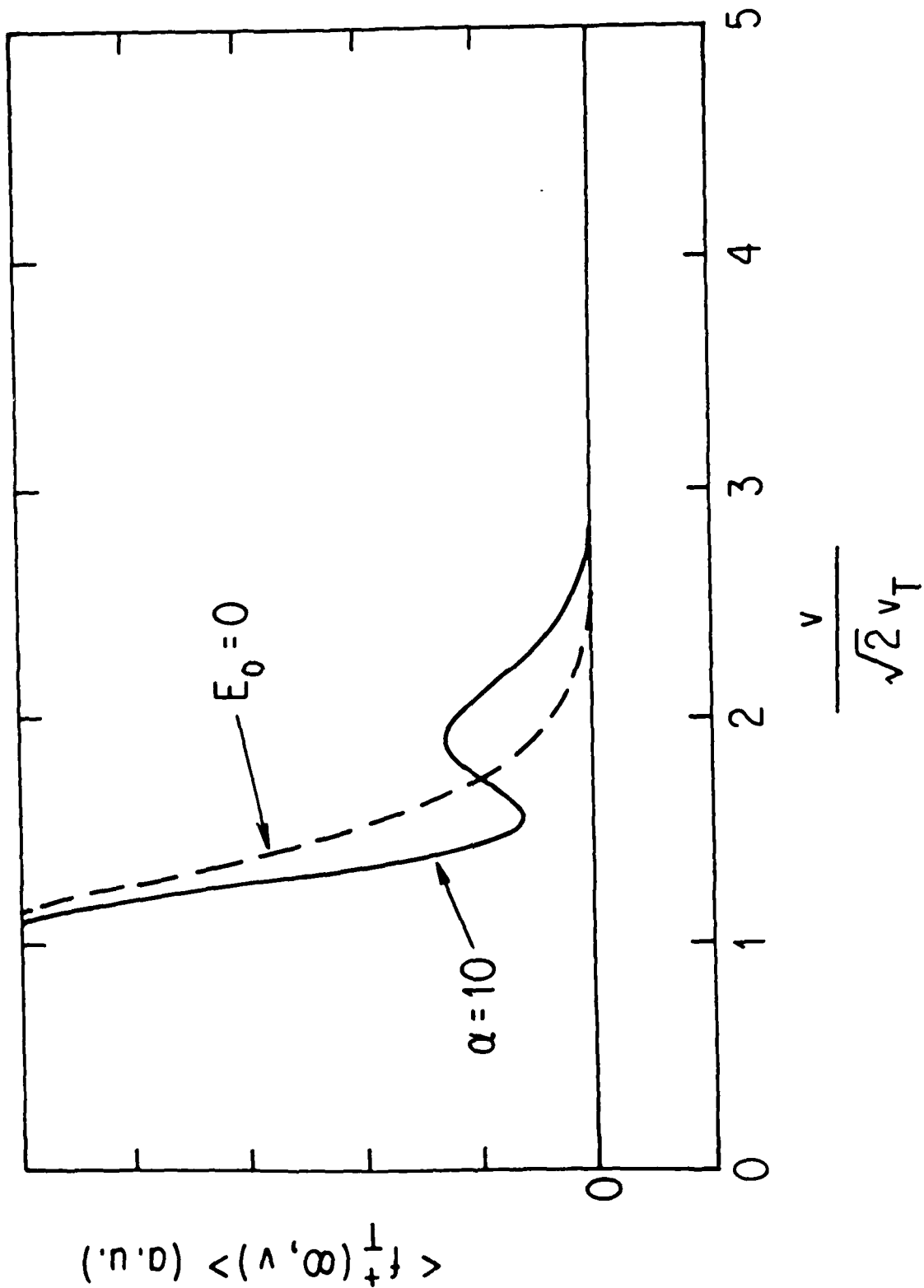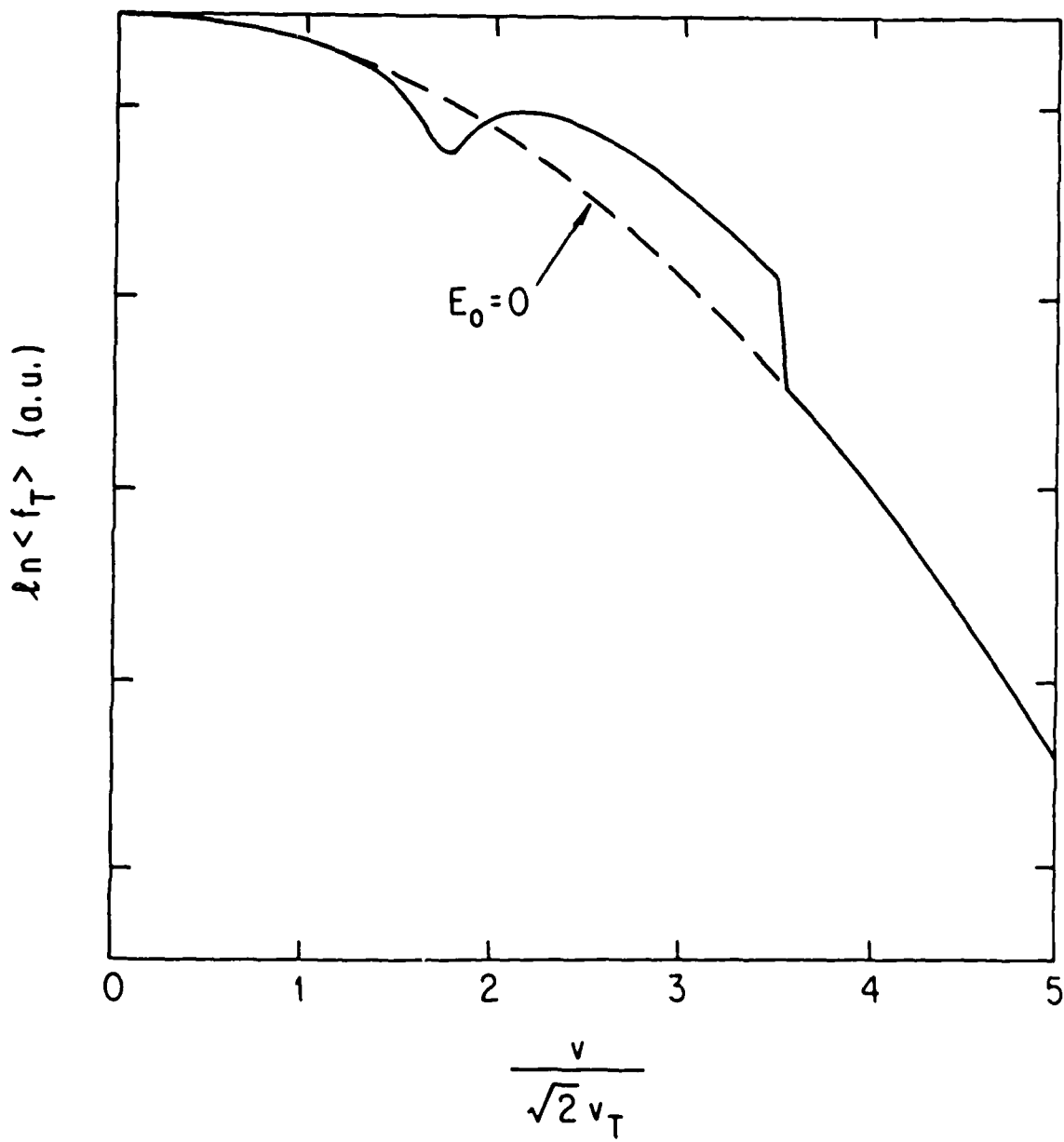
Fig. 12

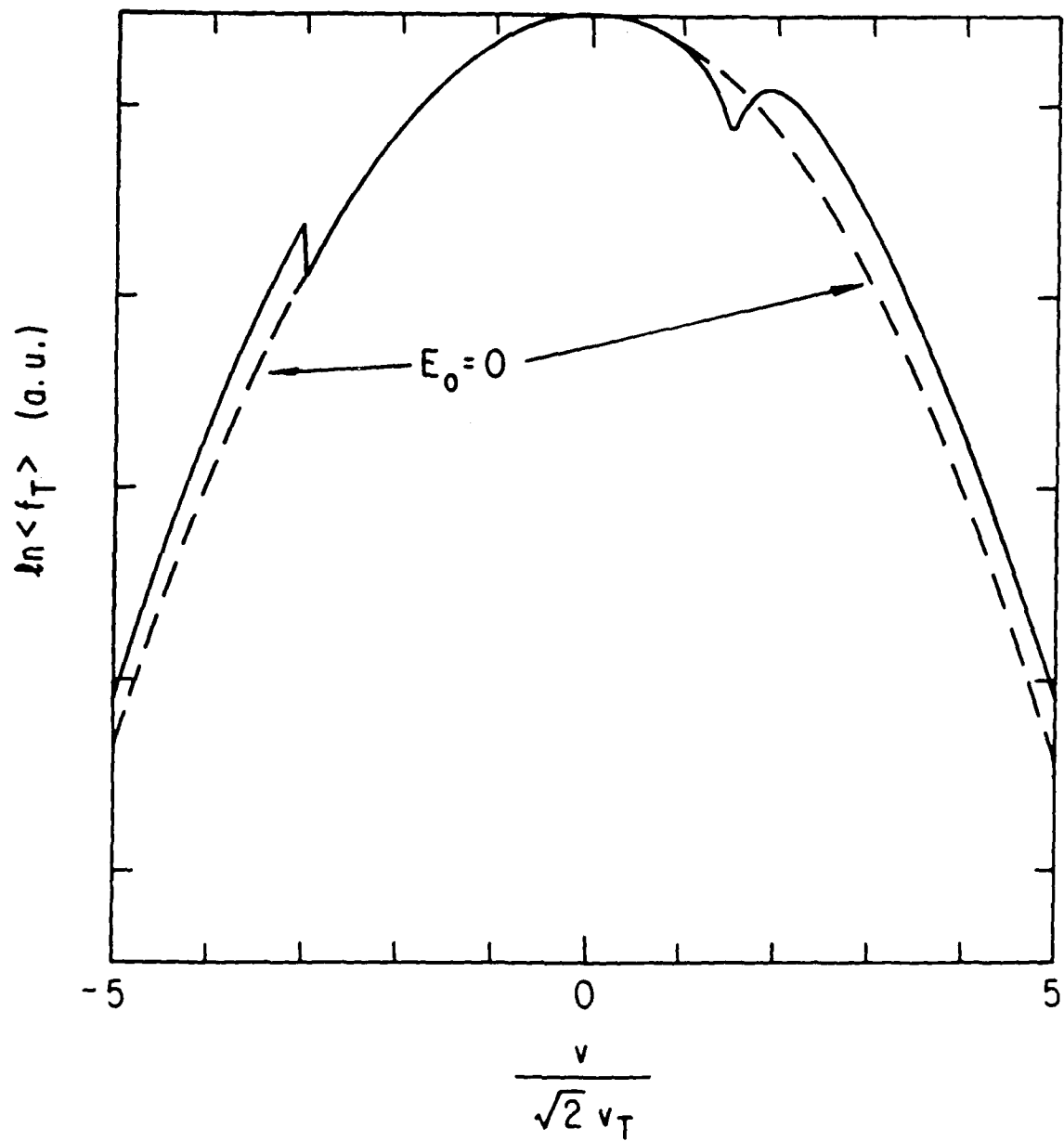Fig. 13

PPG-1064 "The Focusing of a Relativistic Electron Beam Using a Preformed Ion Channel", S. Wilks, J.M. Dawson, and T. Katsouleas, submitted to Phys. Rev. A, April 1987.

PPG-1065 "On MHD Intermediate Shocks," C. C. Wu, to be published to Geophys. Res. Letts., May, 1987.

PPG-1066 "Development of a Mass - Sensitive Ion Energy Analyzer" G. Hairapetian and R. Stenzel, submitted to R.S.I. May, 1987.

PPG-1067 "The MHD Intermediate Shock Interaction with an Intermediate Wave: Are Intermediate Shocks Physical?" by C. C. Wu, May, 1987.

PPG-1068 "Linear Instabilities in Multicomponent Plasmas and their Consequences on the Auroral Zone" D. Schriver and M. Ashour-Abdalla submitted to J.J.R., May, 1987.

PPG-1069 "Cosmic Ray Acceleration: A Plasma Physicist's Perspective" C.F. Kennel, submitted to Inter. "Rosenbluth Symposium", on Dynamics of Particles and Plasmas, Austin, Texas, February 5-6, 1987.

PPG-1070 "Ray Tracing Analysis of LH Fast Waves in CCT", T.K. Mau, K.F. Lai, R.J. Taylor, submitted to the 7th APS Conference, Kissimmee Florida, May 4-6 1987.

PPG-1071 "Combined Wiggler and Solenoidal Field Effects In Free Electron Laser and Electron Cyclotron Maser," T. H. Kho and A. T. Lin, invited paper presented by A. T. Lin at the Fourth International Symposium on Gyrotron and Free Electron Laser, Chegdu, People's Republic of China, May, 1987.

PPG-1072 "MHD Flow in a Curved Pipe," F. Issicci, N.G. Ghoniem, and I. Catton, submitted to Phys. Fluids, June 1987.

PPG-1073 "The New Roles of Cavitones in Inhomogeneous Plasmas Under Strong Electromagnetic Irradiation" T. Tanikawa, Ph.D Dissertation.

PPG-1074 "Progess Report on Pisces: Plasma-Surface Interactions and Materials Research" Pisces Group *R. W. Conn, D. M. Gobel, Y. Hirooka, B. LaBombard W. K. Leung and R. Nygren. June, 1987.

PPG-1075 "Self-Consistent Modification of a Fast Tail Distribution by Resonant Fields in Nonuniform Plasmas," G. J. Morales, M. M. Shoucri and J. E. Maggs, submitted to Phys. of Fluids, June, 1987.

PPG-1076 "Theory and Simulations on Beat Wave Excitation of Relativistic Plasma Waves," W. B. Mori, Ph.D. dissertation, June 1987.

PPG-1077 "Equilibrium and Wave Properties of Two-Dimensional Ion Plasmas", G.J. Morales and S.A. Prasad, submitted to Phys. of Fluids, June, 1987

PPG-1078   "Observation of Stable Axisymmetric Mirror Equalibrium at Arbitrary
           β", A. Kuthi, H. Zwi, L. Schmitz and A.Y. Wong, submitted to
           Phys. PRL., June 1987.

PPG-1079   "Stability of a Rotating Field Generated Mirror Equilibrium", A.
           Kuthi, submitted Phys. Lett. A, July 1987.

PPG-1080   "Dynamical Computer Simulation of the Evolution of a 1-D Dislocation
           Pileup", R. Amodeo, and N.M. Ghoniem, submitted Int'l. J. of Engr.
           Sci., July 1987.

PPG-1081   "International Collaboration in Theory and Modeling of Radiation
           Damage in Fusion Materials Utilizing Supercomputers", N.M. Ghoniem,
           ed., July 1987.

PPG-1082   "Trip Report - Plasma Physics Division Meeting , European Physical
            Society", Burton D. Fried,   Madrid, June 22-26, 1987 .

PPG-1083   "Nature and the Nonlinear Evolution of Electrostatic Waves
           Associated With The AMPTE Solar Wind Releases", N. Omidi, K.
           Akimoto, D.A. Gurnett and R.R. Anderson, submitted JGR, June 11,
           1987.

PPG-1084   "Alt-I Pump Limiter Experiments", D. M. Goebel, R.W. Conn, G.A.
           Campbell, W.K. Leung*, K.H. Dippel, K.H. Finken, G.H. Wolf, G.J.
           Thomas, A.E. Pontau, W. Hsu, submitted to INTOR Design Report June
           1987.

PPG-1085   "Technical Assessment of Plasma-Interactive Options for Claddings
           and Attachments for Steady State", (TAPIOCA)", Matthew C. Carroll
           August 1986.

PPG-1086   "The Use of Liquid Metal Coolants in the Thermal Hydraulic Design of
           the First Wall and Blanket of High Power Density Fusion Reactors."
           M. Hasan, and N. Ghoniem, submitted to Nuclear Engineering and
           Design/Fusion , August 1987.

PPG-1087   "Core Flow Solution of the Liquid Metal MHD Equations in a
           Variable-Radius Pipe " M.S.Tillack, July 29, 1987.

PPG-1088   "RF Heating the Ionosphere," G. J. Morales, presented at the Seventh
           APS Topical Conference, Kissimmee, Florida, May 4-6, 1987.

PPG-1089   "Self-Consistent Modification of a Fast Tail Distribution by
           Resonant Fields in Nonuniform Plasmas," G.J. Morales, M.M. Shoucri,
           J.E. Maggs, August 5, 1987.

END

9-87

DTIC